

# Sigma Delta quantization for images\*

He Lyu, Rongrong Wang

Michigan State University

May 19, 2020

## Abstract

In this paper, we propose the first adaptive quantization method for direct digital image acquisition that yields a better information conversion rate than the state-of-the-art method in cameras. This new method allows a rich color-palette to be reconstructed by using extremely low bits for each pixel and therefore is beneficial for capturing scenes with high-contrast. The work is motivated by recent results on super-resolution for sparse signals, but is free from the usual separation requirement between spikes. We assume natural images are of small TV norms of order 1 or 2, and design an appropriate reconstruction algorithm that reduces the reconstruction error from the known  $O(\sqrt{P})$  to  $O(\sqrt{s})$  where  $P$  is the number of pixels and  $s$  is the number of edges in the image. Our numerical experiments confirm these theoretical findings and further show that a dramatic increase in the photo quality can be achieved when the photo is taken in a dark environment.

## 1 Introduction

### 1.1 Quantization

In digital signal processing, quantization is the step of converting a signal's real-valued samples into a finite string of bits. As the first step in digital processing, it plays a crucial role in determining the information conversion rate and the reconstruction quality. Mathematically, given a signal class  $\mathcal{S} \subseteq \mathbb{R}^N$  and a fixed codebook  $\mathcal{C}$ , the goal of the quantization is to find for every signal  $x$  in  $\mathcal{S}$  a codebook representation  $q \in \mathcal{C}$  so that it can be stored digitally. We use  $Q$  to denote the quantization map between the signal space  $\mathcal{S}$  and the codebook  $\mathcal{C}$

$$Q : \mathcal{S} \rightarrow \mathcal{C} : x \rightarrow q.$$

---

\*PPA no. 63/024,861

Quantization schemes are usually equipped with reconstructing algorithms, that can reconstruct the original signal from the encoded bits. To ensure practicability, the reconstruction algorithms have to be solvable in polynomial times. More explicitly, the algorithm, denoted by  $\Delta$ , should be able to reconstruct every signal  $x \in \mathcal{S}$  from their encoded vector  $q$  in polynomial time up to some small distortion

$$\text{Distortion} := \|\hat{x} - x\|_2 \equiv \|\Delta(q) - x\|_2.$$

For a given signal class  $\mathcal{S}$ , we define the optimal quantization  $Q$  to be the one optimizing the bit rate distortion defined as the minimal possible distortion under a fixed bit budget. Let  $R$  be the fixed budget, among all codebook  $\mathcal{C}$  representable in  $R$  bits, the optimal quantization  $Q$  is the one that minimizes the minimax distortion

$$\hat{Q} = \arg \min_{Q: \mathcal{S} \rightarrow \mathcal{C}, |\mathcal{C}|=2^R} \min_{\Delta \in \mathcal{D}} \max_{x \in \mathcal{S}} \|\Delta \circ Q(x) - x\|_2,$$

where  $\mathcal{D}$  is the class of polynomial time decoders.

If the signal class  $\mathcal{S}$  forms a compact metric space, one can find the optimal quantizer using an information theoretical argument. Given a fixed approximation error  $\epsilon$ , one can find infinitely many  $\epsilon$ -nets of  $\mathcal{S}$ . The smallest possible cardinality of the  $\epsilon$ -nets is called the covering number  $N(\epsilon)$ . Suppose such an optimal  $\epsilon$ -net is given, we define the quantization  $Q$  as the map that sends every point in  $\mathcal{S}$  to the center of the  $\epsilon$ -ball containing this point. Using the binary representation, the number of bits needed to encode the centers is  $R = \log_2 N(\epsilon)$ . This relation reduces to  $\epsilon \sim 2^{-R/d}$  when  $\mathcal{S}$  is the  $\ell_2$  ball in  $\mathbb{R}^d$  (see, e.g., [7, 33, 39]), where  $\sim$  means the two sides are equal to each other up to some constant. We call this relation  $\epsilon \sim 2^{-R/d}$  the exponential relation, which is the best decay rate for  $\epsilon$  as  $R$  increases. However, this optimal quantization scheme suffers from the following impracticality. 1. unless  $\mathcal{S}$  has a regular shape, finding the  $\epsilon$ -covering for  $\mathcal{S}$  suffers from the curse of dimensionality. 2. the scheme cannot be operated in an online manner, as the nearest center of  $x$  can only be found after all samples of  $x$  have been received. 3. If extra samples come in, the  $\epsilon$ -net needs to be recalculated.

These concerns inspire people to impose the following practical requirements on the quantizer  $Q$ .

- the quantization  $q$  should have the same size as the signal  $x$ ;
- $Q$  should quantize each entry of  $x$  to an entry of  $q$  in an online manner, which means  $q_i$  (the  $i^{\text{th}}$  entry of  $q$ ) only depends on the historical inputs  $x_1, \dots, x_i$  not the future ones  $x_{i+1}, \dots$ ;
- the alphabets  $\mathcal{A}_i$  for each  $q_i$  are the same and fixed in advance, i.e.,  $\mathcal{A}_1 = \mathcal{A}_2 = \dots = \mathcal{A}_n = \mathcal{A}$ . Together they form the codebook  $\mathcal{C} = \mathcal{A}^n$ ;
- as the quantization is implemented in the analog hardware, the mathematical operations should be kept as simple as possible. In particular, addition and subtraction are more preferred than multiplication and division due to the ease of circuit implementation.

Here, for simplicity, we choose alphabet  $\mathcal{A}$  from the class of finite equal-spacing grids with step-size  $\delta$ ,

$$\mathcal{A}_\delta = \{c + J\delta, c \in \mathbb{R}, J \in \mathbb{Z}, J_1 \leq J \leq J_2\}. \quad (1.1)$$

## 1.2 MSQ and Sigma Delta quantization

We introduce the existing quantization schemes directly in the context of image quantization. Let  $X \in [a, b]^{N, N}$  store the pixel values of a grayscale image. Without any ambiguity, we will refer to the matrix  $X$  as the image.

**Memoryless Scalar Quantization (MSQ):** Suppose the alphabet  $\mathcal{A} = \mathcal{A}_\delta$  is defined as in (1.1), the scalar quantization,  $Q_{\mathcal{A}} : [a, b] \rightarrow \mathcal{A}$  quantizes a given scalar by rounding it off to the nearest element in the alphabet

$$Q_{\mathcal{A}}(z) \in \arg \min_{v \in \mathcal{A}} |v - z|.$$

The Memoryless Scalar Quantization (MSQ) applies scalar quantization to each sample of the input sequence independently. In terms of image quantization, for a given image  $X$ , MSQ on  $X$  means quantizing each pixel independently

$$\mathcal{A}^{N, N} \ni q = Q_{\mathcal{A}}^{MSQ}(X), \text{ with } q_{i,j} = Q_{\mathcal{A}}(X_{i,j}).$$

Here  $q_{i,j}$  and  $X_{i,j}$  are the  $(i, j)^{\text{th}}$  entry of the quantized and the original images  $q$  and  $X$ , respectively. MSQ is the state-of-the-art quantization in cameras.

**$\Sigma\Delta$  quantization:**  $\Sigma\Delta$  quantization was first proposed for digitalizing bandlimited functions (see, e.g. [26, 16, 22, 40]). It is an adaptive quantization scheme proven to be more efficient than MSQ in a variety of applications [36, 29, 42, 39, 38, 32]. The adaptiveness comes from the fact that it utilizes quantization errors of previous samples to increase the accuracy of the current sample. Suppose the sample sequence is  $y = (y_1, \dots, y_m)$ , the first order  $\Sigma\Delta$  quantization (e.g., [17, 39])  $q = Q_{\mathcal{A}}^{\Sigma\Delta, 1}(y)$  is obtained by running the following iterations

$$\begin{aligned} q_i &= Q_{\mathcal{A}}(y_i + u_{i-1}), \\ (Du)_i &:= u_i - u_{i-1} = y_i - q_i. \end{aligned} \quad (1.2)$$

We can see from the first equation that one quantizes the  $i^{\text{th}}$  input  $y_i$  by first adding to it the historical errors stored in the so-called state variable  $u_{i-1}$  then applying the scalar quantization to the sum. In the second equation, the  $D$  is the forward finite difference operator/matrix, with 1s on the diagonal and -1s on the sub-diagonal. Hence the second equation defines a recurrence relation allowing one to update the state variable  $u_i$ . The scheme defined in (1.2) is the so-called first order quantization scheme because it only uses one step of the historical error,  $u_{i-1}$ . More generally, one can define the  $r^{\text{th}}$  order  $\Sigma\Delta$  quantization

denoted by  $q = Q_{\mathcal{A}}^{\Sigma\Delta,r}(y)$  by involving  $r$  steps of historical errors,  $u_{i-1}, u_{i-1}, u_{i-2}, \dots, u_{i-r}$ . More precisely, each entry  $q_i$  of  $q$  is obtained by

$$q_i = Q_{\mathcal{A}}(\rho_r(u_{i-1}, \dots, u_{i-r}) + y_i),$$

$$(D^r u)_i := y_i - q_i,$$

where  $\rho_r$  is some general function aggregating the accumulated errors  $u_{i-1}, \dots, u_{i-r}$ . The  $r^{\text{th}}$  order finite difference operator is defined via  $D^r u := D(D^{r-1} u)$ .

When using this  $r^{\text{th}}$  order  $\Sigma\Delta$  quantization scheme on a 2D image  $X$ , we need to convert the image  $X$  into sequences. One way to do this is by applying  $\Sigma\Delta$  quantization independently to each column/row,

$$q = Q_{\mathcal{A}}^{\Sigma\Delta,r}(X), \quad q = [q_1, \dots, q_N], \quad q_j = Q_{\mathcal{A}}^{\Sigma\Delta,r}(X_j), \quad j = 1, \dots, N,$$

where  $X_j$  is the  $j^{\text{th}}$  column of  $X$ . As this procedure may create discontinuity across columns, we will propose in Section 2.2 a 2D  $\Sigma\Delta$  quantization scheme that allows a more continuous reconstruction.

### 1.3 The noise shaping effect of the adaptive quantizers

The main advantage of Sigma Delta quantization over MSQ is its adaptive usage of the feedback information. The feedback information helps the quantizer to efficiently use the given bits to maximally store information of special types of signals, such as those with low frequencies [16]. Mathematically, these adaptive quantizers achieve high information conversion rate through the noise-shaping effect on the quantization error, which means the errors of such quantizers are distributed non-uniformly [15, 3, 12]. Figure 1 shows that when inputting the same random sequence, the error spectrum of MSQ is uniform, while that of Sigma Delta quantization is (nearly) linear. This property has the following theoretical explanation. First, the matrix form of definition (1.2) gives an expression of the first order Sigma Delta quantization error  $y - q$

$$y - q = Du, \quad \|u\|_{\infty} \leq \delta/2,$$

where  $\delta$  is the quantization step-size in (1.1) and  $D$  is the finite difference matrix. This is saying that  $y - q \in D(B_{\|\cdot\|_{\infty}}(\delta/2))$ : the quantization error  $y - q$  lies in the  $\ell_{\infty}$  ball of radius  $\delta/2$  reshaped by the operator  $D$ . In case of the  $r^{\text{th}}$  order  $\Sigma\Delta$  quantization ( $r \in \mathbb{Z}_+$ ), we would similarly have

$$y - q = D^r u, \quad \|u\|_{\infty} \leq \delta/2,$$

which means the quantization error  $y - q$  lies in the  $\ell_{\infty}$  ball reshaped by the operator  $D^r$ .

The singular values of  $D^r$  determine the radii of the reshaped  $\ell_{\infty}$  ball containing quantization errors. It was pointed out in [23] that the singular vectors of  $D$  lie almost aligned with the Fourier basis, and the singular values of  $D$  increase with frequencies. Therefore, the low-frequency errors corresponding to smaller singular values of  $D^r$  would be compressed

most. One can numerically verify this unbalanced error reduction effect of  $D^r$  on various sinusoidal frequencies by computing the ratio

$$\rho_r(w) = \frac{\|D^r e^{-iwt}\|_2}{\|e^{-iwt}\|_2}.$$

From the plot of  $\rho_r(w)$  in Figure 2, we can see that the low frequency sinusoids lose more energy after hitting  $D^r$  especially when the quantization order  $r$  is large.

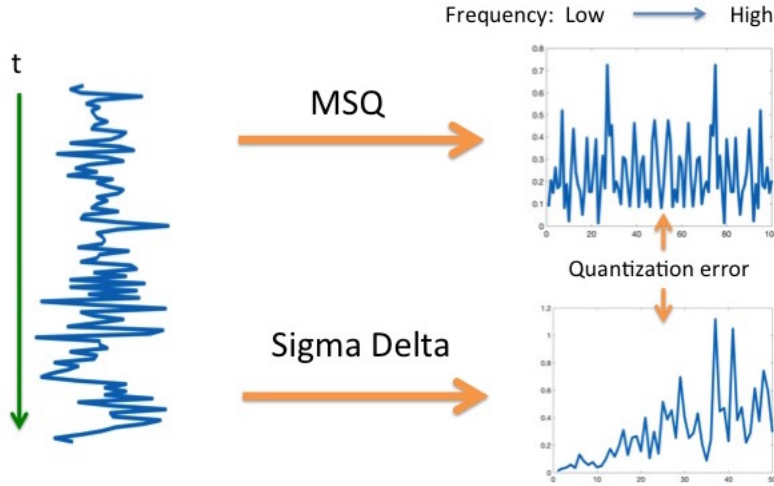


Figure 1: The quantization errors of MSQ and  $\Sigma\Delta$  in the Fourier domain.

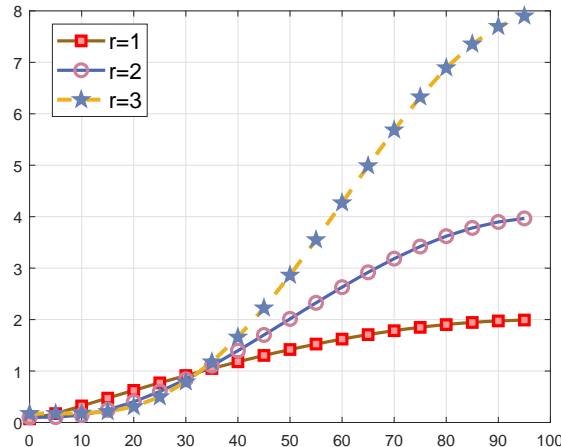


Figure 2: The compression rate of  $D$ ,  $D^2$  and  $D^3$  on exponential functions  $\cos(wt) + i \sin(wt)$  with various frequencies  $w \in [f_0, f_s]$ .

Since Sigma Delta quantization can keep most error away from the low frequency, it is ideal for quantizing low-frequency signals. For instance, dense time samples of audio signals can be deemed as low frequency vectors, and they have indeed been shown to be a good application of Sigma Delta quantization [16, 22]. Images, on the other hand, are not consisted of only low frequencies, as sharp edges have pretty slowly decaying Fourier coefficients. Therefore, it is not obvious whether applying Sigma Delta quantization to images is beneficial.

## 1.4 A quick review of image quantization

Despite the importance of quantization in image acquisition, the simplest MSQ is still the state-of-the-art quantizer in commercial cameras. The major drawback of MSQ is that when the bit-depth (i.e., the number of bits used to represent each pixel) is small, it has a color-banding artifact, i.e., different colors merge together to cause fake contours and plateaus in the quantized image (see (b) of Figure 3). A famous technique called dithering [37, 41] reduces color-banding by randomly perturbing the pixel values (e.g., adding random noise) before quantization. It then breaks artificial contour patterns into the less harmful random noise. However, this random noise is still quite visible ((c) of Figure 3) and a more fundamental issue is that dithering only randomizes the quantization error instead of reducing it. The same amount of errors still exist in the quantized image and will manifest themselves in other ways.

Another method to avoid color-banding is digital halftoning, first proposed in the context of binary printing, where pixel values are converted to 0 or 1 for printing, leading to a possibly severe color-banding artifact. To mitigate it, the digital half-toning was proposed based on the ideas of sequential pixel quantization and error diffusion. Error diffusion means the quantization error of the current pixel will spread out to its neighbours to compensate for the overall under/over-shooting. The decay of energy during spreading is set to empirical values that minimize the overall  $\ell_2$  quantization error of an entire image class. Error diffusion works under a similar assumption as the Sigma Delta quantization that the image intensity is varying slowly and smoothly. In a sense, it trades color-richness with spatial resolution. As dithering, error fusion does not reduce the overall noise but only redistributes it.

## 1.5 Contribution

From the discussion in Section 1.4, we see that both dithering and digital halftoning are only redistributing the quantization error instead of compressing it. In contrast, the method we introduce in this paper achieves a real reduction of the quantization error upon that of MSQ. Explicitly, suppose  $N^2$  is the total number of pixels and  $s$  is the number of pixels representing curve discontinuity (e.g., edges) in the image, our method reduces the quantization error from  $O(N)$  to  $O(\sqrt{s})$ . This is achieved by combining Sigma Delta quantization with an optimization based reconstruction. We observe in the numerical experiment that both the low and high frequency errors are reduced.

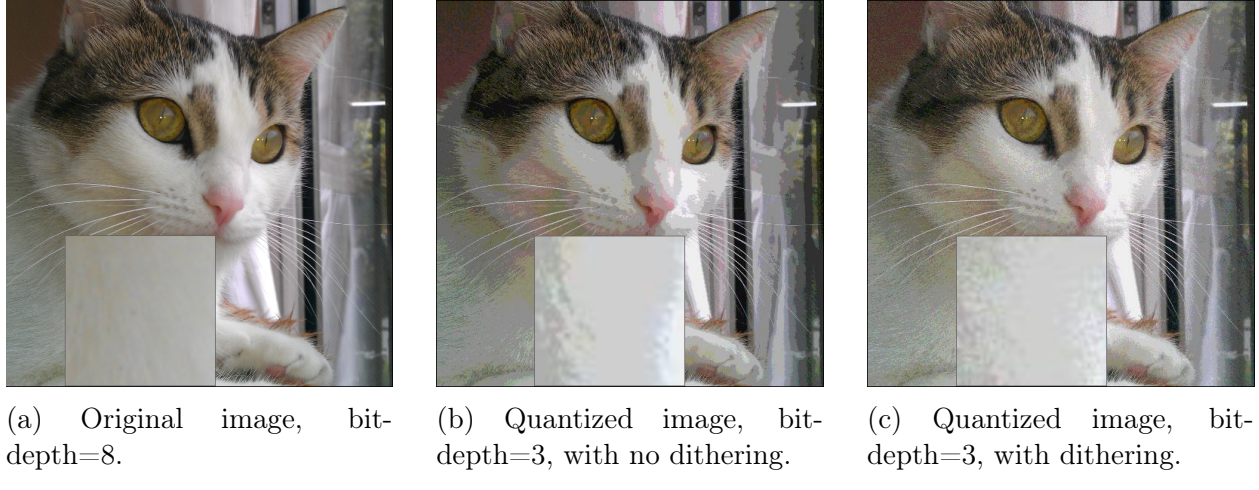


Figure 3: 3-bit MSQ quantization. (a): Original image; (b): Quantized image with MSQ (no dithering), we observe a strong color-banding effect. (c): Quantized image with MSQ + dithering. The image contains observable noisy spots.

Due to the use of the total variation norm in the decoding optimization, our result is closely related to the super-resolution theory [9, 10, 31] in Compressed Sensing, where it is demonstrated that a sparse signal can be super-resolved using  $\ell_1$ -norm minimization if all the spikes in the signal are well-separated. We stress that the error reduction we achieve for the image quantization does not require the edges of the image to satisfy this separation condition, although if the separation condition was met, a further error reduction could be achieved.

Besides Sigma Delta quantization, there exist other adaptive encoders (e.g., Beta encoder [12, 13, 14, 24]). These encoders had been used successfully on 1D audio signals to improve the bit-rate-distortion over MSQ, but none of them was used on images. One major reason is that previous analysis (e.g., [3, 42, 5, 16, 17]) all indicated that these adaptive schemes can only compress low-frequency noise by sacrificing the high-frequency accuracy. While this might be a good idea for audio signals, one does not want to make such a sacrifice when it comes to images. In this paper, we demonstrate that a carefully designed decoder can help retain the high frequency information while compressing the low frequency noises. Therefore, the overall result outperforms MSQ. We only consider Sigma Delta quantization in this paper and leave the study of other adaptive quantizers on images as future work.

Unlike previous works on quantization under frame or Compressed Sensing measurements (see, e.g., [36, 6, 28, 5, 23, 29, 3, 30, 21, 2, 19, 27, 34, 35, 25, 18, 19, 20]), where samples are assumed to be taken by random Gaussian/sub-Gaussian or Fourier measurements, here we allow a direct quantization on each pixel and therefore ensure the maximal practicality.

A by-product of our work is an extension of Sigma Delta quantization to high dimensions. We found that the proposed 2D Sigma Delta quantization can effectively reduce the artifact in the reconstruction while being as fast as the 1D quantization.

## 2 Proposed Method

We propose an adaptive quantization framework for natural images. Given an input image, the quantization workflow involves:

- segmentation: divide the image into columns or rectangular patches;
- quantization: use the existing 1D  $\Sigma\Delta$  quantization in the literature to quantize each column in parallel or use the proposed 2D  $\Sigma\Delta$  quantization (in Section 2.2) to quantize each rectangular patch in parallel;
- reconstruction: run the proposed decoding algorithms (Section 3) to restore the columns or patches and stack them into the final reconstructed image.

### 2.1 The encoders

We consider two types of encoders/quantizers in this paper.

- Encoder 1 ( $Q_{col}$ ): 1D Sigma Delta quantization applied to each column of the image (i.e., column by column quantization)
- Encoder 2 ( $Q_{2D}$ ): 2D Sigma Delta quantization applied to each patch of the image (i.e., patch by patch quantization).

A key question one may ask is the practicality of the proposed adaptive quantizers on commercial cameras. A natural concern is the waiting time. Unlike MSQ that quantizes each pixel in parallel, Sigma Delta quantization can only be performed sequentially, which seems to inevitably introduce extra waiting time. However, this is not the case because current cameras are already using sequential quantization architectures for consistency, energy and size considerations. More specifically, in current cameras, to reduce the number of ADC (Analog to Digital Converters) and save energy, the whole image or a column of pixels are assigned to one ADC, which means these pixels need to wait in a queue to be quantized anyway. This architecture is perfect for Sigma Delta quantization. The only minor change one needs to make is adding an additional memory unit to the circuit.

The structure of the rest of the paper is as follows. In Section 2.2, we introduce the proposed 2D Sigma Delta quantization along with some of its properties. In Section 2.3, we introduce the three image models of interest to this paper. In Section 2.4, we present three decoders associated with each of the three image models and summarize the reconstruction accuracy. The main theorems containing the reconstruction error bounds and their proofs can be found in Section 3. In Section 4, we describe the algorithms one can use to solve the optimization problems in the decoders. Finally in Section 5, we perform numerical experiments to verify the conclusion of the theorems and to provide more evidence of the efficacy of the proposed method.

## 2.2 High dimensional Sigma Delta quantization

Although we can apply 1D  $\Sigma\Delta$  quantization column by column to an image, it is likely to create discontinuities along the horizontal direction. As images are two-dimensional arrays, a two-dimensional quantization scheme is needed here in maintaining the continuity along both vertical and horizontal directions. For this purpose, we propose the first high dimensional Sigma Delta quantization.

In a nutshell, the 1D first order Sigma Delta quantization  $Q_{\mathcal{A}}^{\Sigma\Delta,1}: [a, b]^N \ni y \rightarrow q \in \mathcal{A}^N$  ( $\mathcal{A}$  is the alphabet) is defined by constructing for any  $y \in [a, b]^N$ , two vectors  $q$  (the quantization) and  $u$  (the state variable) of the same length as the input and obeying

- (A1) (boundedness/stability) :  $\|u\|_{\infty} \leq C$ , for some constant  $C$  independent of  $N$ ;
- (A2) (adaptivity):  $u_i = u_{i-1} + y_i - q_i, \forall i$ , where  $u_i, y_i, q_i$  being the  $i^{\text{th}}$  component of the vectors  $u, x$  and  $q$ , respectively;
- (A3) (causality):  $q$  only depends on the history of  $x$ , that is  $q_i = f(y_i, y_{i-1}, \dots, y_1)$ , for any  $i$  and some function  $f$ .

We now extend these conditions to two dimensions, the extensions to higher dimensions are similar. The Sigma Delta quantization in 2D is well defined and denoted as  $Q_{\mathcal{A},2D}^{\Sigma\Delta}: [a, b]^{N,N} \ni y \rightarrow q \in \mathcal{A}^{N,N}$ , if we can construct or any  $y \in [a, b]^{N \times N}$ , two  $N \times N$  matrices  $q$  and  $u$  satisfying a similar set of three conditions:

- (A1')  $\|u\|_{\max} \leq C$  ( $\|\cdot\|_{\max}$  denotes the entry-wise maximum of a matrix);
- (A2')  $u_{i,j} = u_{i,j-1} + u_{i-1,j} - u_{i-1,j-1} + y_{i,j} - q_{i,j}$  which has a matrix representation  $DuD^T = y - q$ ; and
- (A3')  $q_{i,j} = f(\{y_{i',j'}\}_{i' \leq i, j' \leq j})$ .

Provided that the quantization alphabet is large enough, one can show that the  $u$  and  $q$  that satisfy (A1')-(A3') can be constructed through the recursive formula

$$\begin{aligned} q_{i,j} &= Q_{\mathcal{A}}(u_{i,j-1} + u_{i-1,j} - u_{i-1,j-1} + y_{i,j}), \\ u_{i,j} &= u_{i,j-1} + u_{i-1,j} - u_{i-1,j-1} + y_{i,j} - q_{i,j}, \end{aligned} \tag{2.1}$$

where  $i, j > 1$ . When  $i = 1$  or  $j = 1$ , the first row and column can be initialized using the 1D  $\Sigma\Delta$  quantization. In the extreme case when the bit-depth is 1, there might not exist a pair of  $u$  and  $q$  obeying (A1')-(A3') for all  $y \in [a, b]^{N \times N}$ , we leave this as further work. Here we focus on the case when bit-depth  $\geq 2$ . We first show in Proposition 2.1 that a stable 2D Sigma Delta quantization exists and then in Proposition 2.2 that the uniform alphabet with a certain step-size has the optimal stability among all alphabets of the same bit-depth.

**Proposition 2.1.** *For a given 2D array  $y \in [a, b]^{N,N}$  and bit-depth  $d \geq 2$ , there exists an alphabet  $\mathcal{A}$  such that  $u$  and  $q$  generated by (2.1) satisfy (A1')-(A3') with  $C = \frac{b-a}{2(2^d-3)}$ .*

*Proof.* Without loss of generality, assume for all  $1 \leq i, j \leq N$ ,  $a \leq y_{i,j} \leq b$ , with some constant  $a \leq b$ . Let  $C = \frac{b-a}{2(2^d-3)}$ , and create the alphabet as

$$\mathcal{A} = \{a-2C, a, a+2C, \dots, b, b+2C\}.$$

Then  $|\mathcal{A}| = \frac{b+2C-(a-2C)}{2C} + 1 = 2^d$ . Now we use the second principle of induction to show that  $u$  generated by (2.1) satisfies  $\|u\|_\infty \leq C$ .

- Induction hypothesis: if for all the pairs  $(m, n)$  such that  $m \leq i$ ,  $n \leq j$ ,  $m+n < i+j$ ,  $|u_{m,n}| \leq C$ , then  $|u_{i,j}| \leq C$ .
- Base case:  $|u_{1,1}| = |y_{1,1} - q_{1,1}| = |y_{1,1} - Q_{\mathcal{A}}(y_{1,1})| \leq C$ .
- Induction step: if  $i = 1$ ,  $q_{i,j} = Q_{\mathcal{A}}(y_{i,j} + u_{i,j-1})$ , by induction hypothesis we have  $a-C \leq y_{i,j} + u_{i,j-1} \leq b+C$ , thus  $|u_{i,j}| = |y_{i,j} + u_{i,j-1} - q_{i,j}| \leq C$ . The same reasoning follows when  $j = 1$ .

If  $i, j \geq 2$ , by induction hypothesis  $a-3C \leq y_{i,j} + u_{i,j-1} + u_{i-1,j} - u_{i-1,j-1} \leq b+3C$ , we also have  $|u_{i,j}| = |y_{i,j} + u_{i,j-1} + u_{i-1,j} - u_{i-1,j-1} - q_{i,j}| \leq C$ .

□

Next we show that the stability constant  $C = \frac{b-a}{2(2^d-3)}$ , corresponding to the uniform alphabet

$$\mathcal{A} = \{a-2C, a, a+2C, \dots, b, b+2C\}$$

used in the above proposition is optimal.

**Proposition 2.2.** *For a fixed bit-depth  $d \geq 2$ , the alphabet  $\mathcal{A}$  for the 2D  $\Sigma\Delta$  quantization given in Proposition 2.1 is optimal, in the sense that let  $\tilde{C}$  be the stability constant of any other  $d$ -bit alphabet  $\tilde{\mathcal{A}}$  (not necessarily equal-spaced), then it is necessary that  $\tilde{C} \geq C$ .*

*Proof.* Prove by contradiction, assume there exists a  $d$ -bit alphabet  $\tilde{\mathcal{A}}$  whose stability constant is smaller, i.e.,  $\tilde{C} < C$ . Let the alphabet  $\tilde{\mathcal{A}}$  be  $c_1 < c_2 < \dots < c_N$ , with  $N = 2^d$ . Assume  $c_1 < \dots < c_i < a \leq c_{i+1} < \dots < c_j \leq b < c_{j+1} < \dots < c_N$ , note that there is no restriction on the range of alphabet, that is, it is possible that  $a \leq c_1$  or  $b \geq c_N$ . Also, denote the largest interval length in the alphabet within  $[a, b]$  as  $2\tilde{I} = \max\{2I, b - c_j\}$  and  $2I = \max\{c_{i+2} - c_{i+1}, \dots, c_j - c_{j-1}\}$ . The case  $d \geq 3$  is easier than  $d = 2$ , so we first prove the case  $d \geq 3$ .

For  $d \geq 3$ , we start by proving that there are at least two elements in the alphabet that are within  $[a, b]$ , so  $I$  is well defined. Notice that  $C = \frac{b-a}{2(2^d-3)} < \frac{b-a}{10}$ , if there is zero or only one  $c_\ell$  between  $a, b$ , i.e.,  $a \leq c_\ell \leq b$ , then we can choose  $a \leq y_{1,1} \leq b$  properly such that  $|y_{1,1} - Q_{\mathcal{A}}(y_{1,1})| \geq \frac{b-a}{4} > C > \tilde{C}$ , which leads to a contradiction.

Next, consider the following cases:

- $a \leq c_1$  or  $b \geq c_N$ , under this assumption one of the following two cases must hold: 1)  $a \leq c_1$  and  $c_1 - a \geq b - c_N$  or 2)  $b > c_N$  and  $b - c_N > c_1 - a$ . A closer look indicates that these two cases are exact the same upon exchanging the roles of  $a$  and  $b$  hence they share the same proof. Without loss of generality, we assume case 1 hold:  $a \leq c_1$  and  $c_1 - a \geq b - c_N$ . Next, specify the following sub-cases:

(a)  $c_N \leq b$ , let  $[c_\ell, c_{\ell+1}]$  be the largest interval in  $\tilde{\mathcal{A}}$  for some  $\ell$ , i.e.,  $c_{\ell+1} - c_\ell = 2I$ . Choose  $y_{1,1} = \frac{c_\ell + c_{\ell+1}}{2} - \epsilon$ ,  $y_{1,2} = y_{2,1} = c_\ell + 2\epsilon$  with small enough  $\epsilon$  such as  $10^{-10}(C - \tilde{C})$  and  $y_{2,2} = a$ , this leads to  $u_{1,1} = I - \epsilon$ ,  $u_{1,2} = u_{2,1} = -I + \epsilon$ , then  $q_{2,2} = Q_{\mathcal{A}}(y_{2,2} + u_{1,2} + u_{2,1} - u_{1,1}) = Q_{\mathcal{A}}(a - 3I + 3\epsilon)$ , the quantization error

$$\begin{aligned}
|u_{2,2}| &= |y_{2,2} + u_{1,2} + u_{2,1} - u_{1,1} - q_{2,2}| \\
&= |Q_{\mathcal{A}}(a - 3I + 3\epsilon) - (a - 3I + 3\epsilon)| \\
&= c_1 - a + 3I - 3\epsilon \\
&\geq c_1 - a + \frac{3}{2} \cdot \frac{c_N - c_1}{2^d - 1} - 3\epsilon \\
&\geq c_1 - a + \frac{3}{2} \cdot \frac{b - a - 2(c_1 - a)}{2^d - 1} - 3\epsilon \\
&\geq \frac{3(b - a)}{2(2^d - 1)} - 3\epsilon \\
&\geq \frac{b - a}{2(2^d - 3)} - 3\epsilon \\
&= C - 3\epsilon > \tilde{C}.
\end{aligned}$$

The second inequality used the assumption  $c_1 - a \geq b - c_N$ , the third one used  $c_1 - a \geq 0$  and  $d \geq 3$ . Then this contradicts the assumption  $\|u\|_{\max} \leq \tilde{C}$ .

(b)  $c_N > b$  and  $c_{j+1} - c_j < 3(b - c_j)$ . If  $2\tilde{I} = \max\{2I, b - c_j\} = b - c_j$ , let  $y_{1,1} = c_j + \tilde{I} - \epsilon$ ,  $y_{1,2} = y_{2,1} = \frac{c_{j+1} + c_j}{2} - \tilde{I} + 2\epsilon \leq b$  with sufficiently small  $\epsilon$  as in (a) and  $y_{2,2} = a$ , then  $u_{1,1} = \tilde{I} - \epsilon$ ,  $u_{1,2} = u_{2,1} = -\frac{c_{j+1} - c_j}{2} + \epsilon < -\tilde{I} + \epsilon$ . If  $2\tilde{I} = 2I$ , we can choose  $y_{1,1}, y_{1,2}, y_{2,1}$  as in (a) such that  $u_{1,1} = \tilde{I} - \epsilon$ ,  $u_{1,2} = u_{2,1} = -\tilde{I} + \epsilon$ . In both cases, let  $y_{2,2} = a$ , we have  $y_{2,2} + u_{1,2} + u_{2,1} - u_{1,1} \leq a - 3\tilde{I} + 3\epsilon < c_1$ ,

$q_{2,2} = Q_{\mathcal{A}}(y_{2,2} + u_{1,2} + u_{2,1} - u_{1,1}) = c_1$ , the quantization error at  $q_{2,2}$  is

$$\begin{aligned}
|u_{2,2}| &= |c_1 - (y_{2,2} + u_{1,2} + u_{2,1} - u_{1,1})| \\
&\geq c_1 - a + 3\tilde{I} - 3\epsilon \\
&\geq c_1 - a + \frac{3}{2} \cdot \frac{b - c_1}{2^d - 1} - 3\epsilon \\
&\geq c_1 - a + \frac{3}{2} \cdot \frac{b - a - (c_1 - a)}{2^d - 1} - 3\epsilon \\
&\geq \frac{3(b - a)}{2(2^d - 1)} - 3\epsilon \\
&\geq \frac{b - a}{2(2^d - 3)} - 3\epsilon \\
&= C - 3\epsilon > \tilde{C}.
\end{aligned}$$

This leads to a contradiction.

(c)  $c_N > b$  and  $c_{j+1} - c_j \geq 3(b - c_j)$ . If we choose  $y_{1,1} = \frac{b + c_j}{2} - \epsilon$  with some small  $\epsilon$  and  $y_{1,2} = b$ , then  $u_{1,1} = \frac{b - c_j}{2} - \epsilon$ ,  $u_{1,2} = \frac{3}{2}(b - c_j) - \epsilon \leq \tilde{C}$ . Since it holds for arbitrary small  $\epsilon$ , we must have  $b - c_j \leq \frac{2}{3}\tilde{C}$ . This gives  $b - \frac{2}{3}\tilde{C} \leq c_j \leq b$  and  $2I \geq \frac{c_j - c_1}{j - 1} \geq \frac{b - \frac{2}{3}\tilde{C} - c_1}{2^d - 2}$ , where the last inequality is due to the assumption  $c_N > b$  so that  $j \leq N - 1$ . Same as in (a), we can choose  $y_{1,1}, y_{1,2}, y_{2,1}$  properly and  $y_{2,2} = a$ , such that  $u_{1,1} = I - \epsilon$ ,  $u_{1,2} = u_{2,1} = -I + \epsilon$ , provided that  $\epsilon$  is small enough. Then the quantization error at  $q_{2,2} = Q(a - 3I + 3\epsilon) = c_1$  is

$$\begin{aligned}
|u_{2,2}| &= |Q_{\mathcal{A}}(a - 3I + 3\epsilon) - (a - 3I + 3\epsilon)| \\
&= c_1 - a + 3I - 3\epsilon \\
&\geq c_1 - a + \frac{3}{2} \cdot \frac{b - \frac{2}{3}\tilde{C} - c_1}{2^d - 2} - 3\epsilon \\
&\geq c_1 - a + \frac{3}{2} \cdot \frac{b - a - \frac{b-a}{3(2^d-3)} - (c_1 - a)}{2^d - 2} - 3\epsilon \\
&\geq \frac{3}{2} \cdot \frac{b - a - \frac{b-a}{3(2^d-3)}}{2^d - 2} - 3\epsilon \\
&\geq \frac{b - a}{2(2^d - 3)} - 3\epsilon \\
&= C - 3\epsilon > \tilde{C}.
\end{aligned}$$

This also leads to a contradiction.

- $a > c_1$  and  $b < c_N$ , if we also have  $a > c_2$  and  $b < c_{N-1}$ , then we can easily choose a proper  $a \leq y_{1,1} \leq b$  with quantization error at least  $\max\{2I, c_{i+1} - a, b - c_j\} \geq \frac{b - a}{2(2^d - 4 + 1)} = C > \tilde{C}$ , which leads to contradiction.

Therefore, without loss of generality, assume  $c_1 < a \leq c_2$  and  $c_2 - a \geq b - c_{N-1}$ , similar as above, specify the following sub-cases:

(d)  $c_{N-1} \leq b$ . We first show that for arbitrary constant  $a - 3I < \xi < c_2$ , one can choose  $y_{1,1}, y_{1,2}, y_{2,1}, y_{2,2}$  properly such that  $\xi = y_{2,2} + u_{1,2} + u_{2,1} - u_{1,1}$ . If  $a \leq \xi < c_2$ , set  $y_{1,1} = y_{1,2} = y_{2,1} = c_2$ ,  $y_{2,2} = \xi$ , then  $u_{1,1} = u_{1,2} = u_{2,1} = 0$ ,  $y_{2,2} + u_{1,2} + u_{2,1} - u_{1,1} = \xi$ . If  $a - 3I < \xi < a$ , denote  $w = \frac{a - \xi}{3}$ , then  $0 < w < I$ . Let  $[c_\ell, c_{\ell+1}]$  be the largest interval in  $\tilde{\mathcal{A}}$  for some  $\ell$ , i.e.,  $c_{\ell+1} - c_\ell = 2I$ . Choose  $y_{1,1} = c_\ell + w$ ,  $y_{1,2} = y_{2,1} = c_{\ell+1} - 2w$ ,  $y_{2,2} = a$ , then  $u_{1,1} = w$ ,  $u_{1,2} = u_{2,1} = -w$ , we also have  $y_{2,2} + u_{1,2} + u_{2,1} - u_{1,1} = a - 3w = \xi$ .

Hence whatever  $c_1$  is, we can always obtain the quantization error

$$\begin{aligned}
\max_{a-3I < \xi < c_2} |\xi - Q_{\mathcal{A}}(\xi)| &\geq \frac{1}{3}(c_2 - (a - 3I)) \\
&= \frac{1}{3}(c_2 - a) + I \\
&\geq \frac{1}{3}(c_2 - a) + \frac{1}{2} \cdot \frac{c_{N-1} - c_2}{2^d - 3} \\
&\geq \frac{1}{3}(c_2 - a) + \frac{1}{2} \cdot \frac{b - a - 2(c_2 - a)}{2^d - 3} \\
&\geq \frac{b - a}{2(2^d - 3)} + \left(\frac{1}{3} - \frac{1}{2^d - 3}\right)(c_2 - a) \\
&\geq \frac{b - a}{2(2^d - 3)} \\
&= C > \tilde{C}.
\end{aligned}$$

This leads to a contradiction.

(e)  $c_{N-1} > b$  and  $c_{j+1} - c_j \leq \frac{3}{2}(b - c_j)$ . Similar as in (d), we first show that one can choose  $y_{1,1}, y_{1,2}, y_{2,1}, y_{2,2}$  properly to make  $y_{2,2} + u_{1,2} + u_{2,1} - u_{1,1}$  arbitrary constant between  $a - 3I$  and  $c_2$ . If  $2\tilde{I} = 2I$ , it follows the same reasoning as in (d), here we discuss the case when  $2\tilde{I} = b - c_j$ . If  $a \leq \xi < c_2$ , let  $y_{1,1} = y_{1,2} = y_{2,1} = c_j$ ,  $y_{2,2} = \xi$ , then  $y_{2,2} + u_{1,2} + u_{2,1} - u_{1,1} = \xi$ . If  $a - 3\tilde{I} < \xi < a$ , denote  $w = a - \xi$ , then  $0 < w < 3\tilde{I}$ , we specify the following sub-cases: i) if  $0 < w \leq \tilde{I}$ , let  $y_{1,1} = c_j + w$ ,  $y_{1,2} = y_{2,1} = c_j - w$ ,  $y_{2,2} = a$ , then  $u_{1,1} = w$ ,  $u_{1,2} = u_{2,1} = 0$ ,  $y_{2,2} + u_{1,2} + u_{2,1} - u_{1,1} = a - w = \xi$ ; ii) if  $\tilde{I} < w \leq 2\tilde{I}$ , let  $y_{1,1} = c_j + w - \tilde{I}$ ,  $y_{1,2} = c_{j+1} - w$ ,  $y_{2,1} = c_j - (w - \tilde{I})$  and  $y_{2,2} = a$ , then  $u_{1,1} = w - \tilde{I}$ ,  $u_{1,2} = -\tilde{I}$ ,  $u_{2,1} = 0$ ,  $y_{2,2} + u_{1,2} + u_{2,1} - u_{1,1} = a - w = \xi$ ; iii) if  $2\tilde{I} < w < 3\tilde{I}$ , let  $y_{1,1} = c_j + w - 2\tilde{I}$ ,  $y_{1,2} = y_{2,1} = c_{j+1} - w + \tilde{I}$  and  $y_{2,2} = a$ , then  $u_{1,1} = w - 2\tilde{I}$ ,  $u_{1,2} = u_{2,1} = -\tilde{I}$ ,  $y_{2,2} + u_{1,2} + u_{2,1} - u_{1,1} = a - w = \xi$ .

Therefore, whatever  $c_1$  is, the worst case quantization error can reach

$$\begin{aligned}
\max_{a-3\tilde{I} < \xi < c_2} |\xi - Q_{\mathcal{A}}(\xi)| &= \frac{1}{3}(c_2 - (a - 3\tilde{I})) \\
&= \frac{1}{3}(c_2 - a) + \tilde{I} \\
&\geq \frac{1}{3}(c_2 - a) + \frac{1}{2} \cdot \frac{b - c_2}{2^d - 3} \\
&\geq \frac{1}{3}(c_2 - a) + \frac{1}{2} \cdot \frac{b - a - (c_2 - a)}{2^d - 3} \\
&\geq \frac{b - a}{2(2^d - 3)} + \left(\frac{1}{3} - \frac{1}{2(2^d - 3)}\right)(c_2 - a) \\
&\geq \frac{b - a}{2(2^d - 3)} \\
&= C > \tilde{C}.
\end{aligned}$$

This leads to a contradiction.

(f)  $c_{N-1} > b$  and  $c_{j+1} - c_j > \frac{3}{2}(b - c_j)$ , similar as (c), we must have  $j \leq N - 2$  and  $b - c_j \leq \frac{4}{3}\tilde{C}$ , then

$$\begin{aligned}
\max_{a-3I < \xi < c_2} |\xi - Q_{\mathcal{A}}(\xi)| &= \frac{1}{3}(c_2 - (a - 3I)) \\
&= \frac{1}{3}(c_2 - a) + I \\
&\geq \frac{1}{3}(c_2 - a) + \frac{1}{2} \cdot \frac{b - \frac{4}{3}\tilde{C} - c_2}{2^d - 4} \\
&\geq \frac{1}{3}(c_2 - a) + \frac{1}{2} \cdot \frac{b - a - \frac{2(b-a)}{3(2^d-3)} - (c_2 - a)}{2^d - 4} \\
&\geq \frac{b - a}{2(2^d - 3)} + \left(\frac{1}{3} - \frac{1}{2(2^d - 4)}\right)(c_2 - a) \\
&\geq \frac{b - a}{2(2^d - 3)} \\
&= C > \tilde{C}.
\end{aligned}$$

There also leads to a contradiction.

For the case  $d = 2$ , there are only 4 elements in the alphabet  $\tilde{\mathcal{A}} = \{c_1, c_2, c_3, c_4\}$  with  $c_1 < c_2 < c_3 < c_4$ . Consider the case  $a \leq c_1$  or  $b \geq c_4$ , if there are at least two elements in  $\tilde{\mathcal{A}}$  that are within  $[a, b]$ , the proof follows the same reasoning as  $d \geq 3$ , which has been discussed in (a)-(c). Here we discuss the case that  $a \leq c_1$  and there is only one element in the  $\tilde{\mathcal{A}}$  that

is within  $[a, b]$ , i.e.,  $a \leq c_1 \leq b < c_2 < c_3 < c_4$ . In this case, let  $y_{1,1} = \frac{c_1 + b}{2}$ ,  $y_{1,2} = y_{2,1} = y_{2,2} = a$ , then  $u_{1,1} = \frac{b - c_1}{2}$ ,  $u_{1,2} = u_{2,1} = a - c_1$ ,  $u_{2,2} = a + 2(a - c_1) - \frac{b - c_1}{2} - Q_{\mathcal{A}}(a + 2(a - c_1) - \frac{b - c_1}{2}) = 2(a - c_1) - \frac{b - c_1}{2} \leq \frac{a - c_1}{2} - \frac{b - c_1}{2} = -C$ , hence  $|u_{2,2}| \geq \frac{b - a}{2} = C > \tilde{C}$ , which leads to a contradiction.

Next, we discuss the two remaining cases when both  $a > c_1$  and  $b < c_4$  hold:  $c_1 < a \leq c_2 \leq b < c_3 < c_4$  and  $c_1 < a \leq c_2 < c_3 \leq b < c_4$ , which corresponds to two cases that there are 1 or 2 elements in the alphabet between  $a$  and  $b$ , respectively.

- $c_1 < a \leq c_2 < c_3 \leq b < c_4$ , without loss of generality, assume  $c_2 + c_3 \geq b + a$ . Note that we must have  $c_2 - c_1 < b - a$  since  $\tilde{C} < C = \frac{b - a}{2}$ , combining these two inequalities we get  $c_1 + c_3 > 2a$ , then  $a < \frac{1}{2}(c_1 + c_3) < b$ . Choose some small  $\epsilon$  and the first  $3 \times 3$  entries of  $y$  as

$$y = \begin{pmatrix} \frac{1}{2}(c_3 + c_2) - \epsilon & c_2 & c_2 + 2\epsilon & \dots \\ c_2 & c_2 & \frac{1}{2}(c_1 + c_3) & \dots \\ c_2 + 2\epsilon & \frac{1}{2}(c_1 + c_3) & a & \dots \\ \dots & \dots & \dots & \dots \end{pmatrix}.$$

Provided that  $\epsilon$  is small enough, one can check that the first  $3 \times 3$  entries in  $u$  are as follows

$$u = \begin{pmatrix} \frac{1}{2}(c_3 - c_2) - \epsilon & \frac{1}{2}(c_3 - c_2) - \epsilon & -\frac{1}{2}(c_3 - c_2) + \epsilon & \dots \\ \frac{1}{2}(c_3 - c_2) - \epsilon & \frac{1}{2}(c_3 - c_2) - \epsilon & -\frac{1}{2}(c_2 - c_1) + \epsilon & \dots \\ -\frac{1}{2}(c_3 - c_2) + \epsilon & -\frac{1}{2}(c_2 - c_1) + \epsilon & a - \frac{1}{2}(c_3 + c_2) + 3\epsilon & \dots \\ \dots & \dots & \dots & \dots \end{pmatrix}.$$

By assumption, we have  $c_2 + c_3 \geq b + a$ , then for small enough  $\epsilon$ ,  $|u_{3,3}| \geq \frac{b - a}{2} - 3\epsilon = C - 3\epsilon > \tilde{C}$ , this leads to a contradiction.

- $c_1 < a \leq c_2 < b \leq c_3 < c_4$ , specify the following two cases
  - (i)  $c_2 \geq \frac{b + a}{2}$ , notice that we must have  $c_2 - c_1 < b - a$ , so  $c_1 + c_2 > 2a$ , we can choose  $y_{1,1} = c_2$ ,  $y_{1,2} = y_{2,1} = \frac{1}{2}(c_1 + c_2) + \epsilon$  for sufficiently small  $\epsilon$  and  $y_{2,2} = a$ , then  $u_{1,1} =$

0,  $u_{1,2} = u_{2,1} = -\frac{1}{2}(c_2 - c_1) + \epsilon$  and  $Q_{\mathcal{A}}(y_{2,2} + u_{1,2} + u_{2,1} - u_{1,1}) = Q_{\mathcal{A}}(a - (c_2 - c_1) + 2\epsilon) = c_1$  and  $|y_{2,2} + u_{1,2} + u_{2,1} - u_{1,1} - Q_{\mathcal{A}}(y_{2,2} + u_{1,2} + u_{2,1} - u_{1,1})| = c_2 - a - 2\epsilon \geq \frac{b-a}{2} - 2\epsilon > \tilde{C}$ , which leads to a contradiction.

(ii)  $c_2 < \frac{b+a}{2}$ , also notice that  $c_3 - c_2 < b - a$ , then we can choose  $y$  as follows with some small  $\epsilon$ ,

$$y = \begin{pmatrix} \frac{1}{2}(b + c_2) - \epsilon & c_2 & c_2 + \frac{1}{2}(c_3 - b) + 2\epsilon & \dots \\ c_2 & c_2 & \frac{1}{2}(c_1 + c_3) & \dots \\ c_2 + \frac{1}{2}(c_3 - b) + 2\epsilon & \frac{1}{2}(c_1 + c_3) & a & \dots \\ \dots & \dots & \dots & \dots \end{pmatrix}.$$

Provided that  $\epsilon$  is small enough, the corresponding  $u$  is

$$U = \begin{pmatrix} \frac{1}{2}(b - c_2) - \epsilon & \frac{1}{2}(b - c_2) - \epsilon & -\frac{1}{2}(c_3 - c_2) + \epsilon & \dots \\ \frac{1}{2}(b - c_2) - \epsilon & \frac{1}{2}(b - c_2) - \epsilon & -\frac{1}{2}(c_2 - c_1) + \epsilon & \dots \\ -\frac{1}{2}(c_3 - c_2) + \epsilon & -\frac{1}{2}(c_2 - c_1) + \epsilon & -\frac{c_2 + b}{2} + a + 3\epsilon & \dots \\ \dots & \dots & \dots & \dots \end{pmatrix}.$$

Since  $c_2 \geq a$ , then  $|u_{3,3}| = \frac{c_2 + b}{2} - a - 3\epsilon \geq \frac{b-a}{2} - 3\epsilon > \tilde{C}$ , which leads to a contradiction.  $\square$

**Remark 2.3.** The quantization time of the 2D scheme (2.1) is  $O(N)$ . Because for a fixed  $t \in \{2, 3, \dots, 2N\}$ , all  $u_{i,j}$  with  $i + j = t$  (the points on an anti-diagonal) can be computed in parallel.

**Remark 2.4.** The matrix representation of (2.1) is

$$y - q = DuD^T.$$

It is easy to extend the first order quantization to high orders. If  $r \geq 1$ , the  $r$ -th order quantization obey the matrix form recursive formula

$$y - q = D^r u (D^r)^T.$$

## 2.3 Notation and Assumptions

Throughout, we assume the image  $X$  to be quantized and reconstructed is an  $N \times N$  matrix (everything discussed in the paper can be easily generalized to rectangular matrices),  $X = (\underline{x}_1, \underline{x}_2, \dots, \underline{x}_N) = (\bar{x}_1, \bar{x}_2, \dots, \bar{x}_N)^T$  is the column-wise and row-wise decomposition of  $X$ ,  $D$  is the  $N \times N$  difference matrix with 1s on the diagonal and -1s on the sub-diagonal and  $D_1$  is the circulant difference matrix with an extra -1 on the upper right corner. We denote by  $\|\cdot\|_1$  the entry-wise  $\ell_1$ -norm and by  $\|\cdot\|_\infty$  the entry-wise  $\ell_\infty$ -norm. Also,  $\mathcal{F}_k$  denotes the operator that computes the discrete Fourier coefficient of a vector at frequency  $k$ ,  $F$  is the  $N \times N$  DFT matrix. Let  $F_L$  contain rows of  $F$  with frequencies within  $\{-L, -L+1, \dots, L\}$ , and  $P_L = F_L^* F_L$ . We refer to  $*$  as the circulant convolution operator, and  $A(n) \lesssim B(n)$  means there exists some constant  $c$  independent of  $n$ , such that  $A(n) \leq cB(n)$ .

Our general assumption is that the images satisfy some sparsity property in their gradients. To be more precise, we consider three classes of images each satisfying one of the following three assumptions.

**Assumption 2.1. ( $\beta^{\text{th}}$  order sparsity condition)** Suppose  $X \in [a, b]^{N,N}$  is an image, the columns or rows of  $X$  are piece-wise constant or piece-wise linear. Explicitly, the cardinality of 1<sup>st</sup> order or 2<sup>nd</sup> order differences in each column or row is smaller than the number of pixels: for  $\beta = 1$  or 2, fix  $s < N$ ,

$$\|(D^\beta)^T \underline{x}_i\|_0 \leq s, \quad \forall j = 1, 2, \dots, N, \quad \text{or} \quad \|\bar{x}_j^T D^\beta\|_0 \leq s, \quad \forall j = 1, 2, \dots, N.$$

If  $\beta = 1$ , the columns or rows of image  $X$  are piece-wise constant, if  $\beta = 2$ , they are piece-wise linear.

**Assumption 2.2.** Both columns and rows in  $X$  are piece-wise constant or piece-wise linear. Explicitly, for  $\beta = 1$  or 2, fix  $s < 2N^2$ ,

$$\|(D^\beta)^T X\|_0 + \|X D^\beta\|_0 \leq s.$$

**Assumption 2.3. ( $\beta^{\text{th}}$  order minimum separation condition)**  $X$  satisfies Assumption 2.1. In addition, the  $\beta^{\text{th}}$  order differences of  $X$  in each column or row satisfy the  $\Lambda_M$ -minimum separation condition defined below for some small constant  $M \ll N$ . Explicitly, this means for  $\beta = 1$  or 2,  $\{D_1^\beta \underline{x}_i\}_{i=1,2,\dots,N}$  or  $\{\bar{x}_j^T (D_1^\beta)^T\}_{j=1,2,\dots,N}$  satisfy  $\Lambda_M$ -minimum separation condition, note that here  $D_1$  is the circulant difference matrix.

**Definition 2.1. ( $\Lambda_M$ -minimum)** For a vector  $x \in \mathbb{R}^N$ , let  $S \subset \{1, 2, \dots, N\}$  be its support set, we say that it satisfies  $\Lambda_M$ -minimum separation condition if

$$\min_{s, s' \in T, s \neq s'} \frac{1}{N} |s - s'| \geq \frac{2}{M}, \quad (2.2)$$

where  $|\cdot|$  is the wrap-around distance. As in [31], we use the definition  $C(T, \Lambda_M)$  as the space of trigonometric polynomials of degree  $M$  on set  $T$ , i.e.,

$$C(T, \Lambda_M) = \{f \in C^\infty(T) : f(x) = \sum_{k=-M}^M a_k e^{i2\pi kx}\}.$$

## 2.4 The proposed decoders and their error bounds

Let  $Q$  be encoder  $Q_{col}$  or  $Q_{2D}$  which will be specified in each case, and  $X$  be the image. The proposed decoders for images satisfying different assumptions can be unified in the following framework

$$\hat{X} = \arg \min_Z f(Z, \beta) \quad \text{subject to } \rho(Z, r) \leq c. \quad (2.3)$$

Here  $\beta$  is 1 or 2 depending on whether the image is assumed to be piece-wise constant or piece-wise linear,  $f(Z, \beta)$  is some loss function that encourages sparsity in the gradient under various assumptions,  $r$  is the order of Sigma Delta quantization, and  $\rho(Z, r) \leq c$  is the feasibility constraint determined by the quantization scheme. Under this framework, let  $\hat{X}$  be a solution to (2.3), we obtain reconstruction error bounds of the following type

$$\|\hat{X} - X\|_F \leq C(\beta, r, N, \delta), \quad (2.4)$$

where  $N$  is the size of the image and  $\delta$  is the alphabet step-size.

Now we specify the explicit form of the optimization framework and error bound for each class of images.

- Class 1:  $X$  satisfies Assumption 2.1 with order  $\beta = 1$  or  $2$  and sparsity  $s$ , the encoder is  $r^{\text{th}}$  order ( $r \geq \beta$ )  $Q_{col}$  (Sect. 2.4) with alphabet step-size  $\delta$ , we use the following optimization for reconstruction

$$\hat{X} = \arg \min_Z \|(D^\beta)^T Z\|_1 \quad \text{subject to } \|D^{-r}(Z - Q_{col}(X))\|_\infty \leq \delta/2. \quad (2.5)$$

Theorem 3.1 below shows that the reconstruction error is

$$\|\hat{X} - X\|_F \leq C\sqrt{sN}\delta.$$

- Class 2:  $X$  satisfies Assumption 2.2 with order  $\beta = 1$  or  $2$  and sparsity  $s$ , the encoder is  $Q_{2D}$  (proposed in Sect 2.2) with order  $\beta$  and alphabet step-size  $\delta$ , we use the following optimization

$$\hat{X} = \arg \min_Z \|(D^\beta)^T Z\|_1 + \|ZD^\beta\|_1 \quad \text{subject to } \|D^{-\beta}(Z - Q_{2D}(X))(D^{-\beta})^T\|_\infty \leq \delta/2. \quad (2.6)$$

Theorem 3.4 shows that the reconstruction error is bounded by

$$\|\hat{X} - X\|_F \leq C\sqrt{s}\delta.$$

- Class 3:  $X$  satisfies Assumption 2.3 with order  $\beta = 1$  or  $2$  and sparsity  $s \ll N$ , the encoder is  $r^{\text{th}}$  order Sigma Delta quantization applied to each column:  $Q_{col}$  with alphabet spacing  $\delta$ ,  $r \geq \beta$ . Here we define a new alphabet  $\tilde{A}$  with smaller step-size  $\tilde{\delta} := \frac{2\delta}{(2N)^r}$  to quantize the last  $r$  entries in each column:

$$\tilde{A} := \{a, a + \tilde{\delta}, a + 2\tilde{\delta}, \dots, a + K\tilde{\delta}, b\}, \quad K = \max\{j, a + j\tilde{\delta} < b\}.$$

The total number of boundary bits is of order  $O(\log N)$ , which is negligible comparing to the  $O(N)$  bits needed for the interior pixels. Hence the following feasibility constraint holds:

$$\|D^{-r}(X - Q_{col}(X))_{N-r:N-1,:}\|_\infty \leq \left(\frac{1}{2N}\right)^r \delta.$$

Then we use the following optimization to obtain the reconstructed image  $\hat{X}$ :

$$\begin{aligned} \hat{X} &= \arg \min_Z \|D_1^\beta Z\|_1 \\ \text{subject to } &\begin{cases} \|D^{-r}(Z - Q_{col}(X))\|_\infty \leq \delta/2, \\ \|D^{-r}(Z - Q_{col}(X))_{N-r:N-1,:}\|_\infty \leq \left(\frac{1}{2N}\right)^r \delta. \end{cases} \end{aligned} \quad (2.7)$$

Here  $D^{-r}(Z - Q_{col}(X))_{N-r:N-1,:}$  refers to the last  $r$  rows of  $D^{-r}(Z - Q_{col}(X))$ . The error bound is

$$\|\hat{X} - X\|_F \leq C \frac{M^{r+\beta-2}}{N^{r-3}} \delta.$$

In the following, we discuss Class 1 in Section 3.1, Class 2 in Section 3.2, and Class 3 in Section 3.3.

### 3 Main theorems and proofs

#### 3.1 Class 1: Images with no minimum separation

In this section, we are considering Class 1, where the image  $X$  satisfies Assumption 2.1 with  $\beta = 1, 2$  and the encoder is  $Q_{col}$ , column by column quantization. With this encoder, the decoder (2.5) can be decoupled into columns, with the reconstructions done in parallel.

For each column  $\underline{x} \in \mathbb{R}^N$ , let  $\underline{q}$  be its  $r^{\text{th}}$  order Sigma Delta quantization, i.e.,  $\underline{q} = Q^{\Sigma\Delta,r}(\underline{x})$ ,  $r \geq \beta$ . For simplicity of notation, we use  $x$  and  $q$  to represent  $\underline{x}$  and  $\underline{q}$ , respectively. The decoder (2.5) decouples into columns, for each column the decode reduces to

$$\hat{x} = \arg \min_z \|(D^\beta)^T z\|_1 \text{ subject to } \|D^{-r}(z - q)\|_\infty \leq \delta/2. \quad (3.1)$$

Here  $D$  is the finite difference matrix and  $\delta$  is the quantization step-size. Therefore  $(D^\beta)^T z$  represents the 1<sup>st</sup> order/2<sup>nd</sup> order discrete derivatives in  $z$ . The  $\ell_1$ -norm is used to promote the sparsity of the derivatives corresponding to edges. The ball-constraint is a well known feasibility constraint for Sigma Delta quantization (e.g., [39]).

The following theorem provides the error bound of this decoder.

**Theorem 3.1.** *For first order or second order Sigma Delta decoder (3.1), i.e.,  $\beta = 1$  or  $2$ ,  $r \geq \beta$ , assume the support of  $(D^\beta)^T x$  has cardinality  $s$ , and  $\hat{x}$  is a solution to (3.1), then*

$$\|\hat{x} - x\|_2 \leq C\sqrt{s}\delta. \quad (3.2)$$

**Remark 3.2.** The above error bound is for each column. Putting the error of all columns together as  $\hat{X}$ , we have

$$\|\hat{X} - X\|_F \leq C\sqrt{sN}\delta.$$

**Remark 3.3.** To compare, we specify the quantization error of MSQ and that of the vanilla Sigma Delta decoder. In MSQ, the quantization error for each pixel is  $\delta/2$ . Since the pixels are quantized independently, the total quantization error of the  $N \times N$  image in Frobenius norm is  $N\delta/2$ . Similarly, when using  $\Sigma\Delta$  quantizers ( $Q_{col}$  or  $Q_{2D}$ ) and decoding with the following naive decoder,

$$\hat{X} = \text{Find } Z \text{ subject to } \|D^{-r}(Z - Q_{col}(X))\|_\infty \leq \delta/2,$$

the worse-case error is again  $O(N\delta)$ . This indicates that the TV norm penalty in the proposed decoder (3.1) is playing a key role in reducing the error to  $O(\sqrt{sN}\delta)$ .

### 3.1.1 Proof of Theorem 3.1

Denote  $h = (D^\beta)^T(\hat{x} - x)$ , assume the support set of  $(D^\beta)^T x$  is  $S$  with cardinality  $s$ , the complement of  $S$  is  $S^C$ . Since  $\hat{x}$  is a solution to (3.1), we have

$$\|(D^\beta)^T x\|_1 \geq \|(D^\beta)^T x + h\|_1 \geq \|(D^\beta)^T x\|_1 - \|h_S\|_1 + \|h_{S^C}\|_1,$$

which gives  $\|h_S\|_1 \geq \|h_{S^C}\|_1$ , we can bound the  $\ell_1$ -norm of  $h$  as

$$\|h\|_1 = \|h_S\|_1 + \|h_{S^C}\|_1 \leq 2\|h_S\|_1 \leq 2^{\beta+r+1}s\delta,$$

where the last inequality is due to

$$\|h\|_\infty = \|(D^\beta)^T(\hat{x} - x)\|_\infty = \|(D^\beta)^T D^r D^{-r}(\hat{x} - x)\|_\infty \leq 2^{\beta+r}\delta.$$

Then the following properties hold

$$\|(D^\beta)^T(\hat{x} - x)\|_1 \leq 2^{\beta+r+1}s\delta, \quad \|D^{-\beta}(\hat{x} - x)\|_\infty = \|D^{r-\beta}D^{-r}(\hat{x} - x)\|_\infty \leq 2^{r-\beta}\delta.$$

Note that the inequalities above are bounded in  $\ell_1$ -norm and  $\ell_\infty$  norm, which are dual to each other, we can therefore bound the reconstruction error  $\|\hat{x} - x\|_2$  using

$$\langle \hat{x} - x, \hat{x} - x \rangle = \langle (D^\beta)^T(\hat{x} - x), D^{-\beta}(\hat{x} - x) \rangle \leq 2^{2r+1}s\delta^2.$$

This is equivalent to saying, we have  $\|\hat{x} - x\|_2 \leq C\sqrt{s}\delta$ .

## 3.2 Class 2: Decoding high-dimensional Sigma Delta quantized images

In this section, we consider Class 2, where the image  $X$  satisfies Assumption 2.2 and the encoder is  $Q_{2D}$ . For simplicity, we assume the patch number is 1 (there is only one patch identical to the original image) and  $\beta = 1$ . Results for larger patch numbers or  $\beta = 2$  are similar. The following theorem establishes the error bound for 2D reconstruction of  $X$  from its quantization  $Q_{2D}(X)$  using (2.6).

**Theorem 3.4.** *If the original matrix  $X$  satisfies Assumption 2.2 with order  $\beta = 1$  and sparsity  $s$ , let  $\hat{X}$  be a solution to (2.6), then*

$$\|\hat{X} - X\|_F \leq C\sqrt{s}\delta. \quad (3.3)$$

*Proof.* Denote  $H_1 = D^T(\hat{X} - X)$ ,  $H_2 = (\hat{X} - X)D$ ,  $S_A$  and  $S_B$  are the support sets of  $D^T X$  and  $XD$  respectively, the corresponding complements are  $S_A^C$  and  $S_B^C$ , respectively. By assumption,  $|S_A| + |S_B| \leq s$ . Also notice that

$$\begin{aligned} \|D^T X\|_1 + \|XD\|_1 &\geq \|D^T \hat{X}\|_1 + \|\hat{X}D\|_1 \\ &= \|D^T X + H_1\|_1 + \|XD + H_2\|_1 \\ &\geq \|D^T X\|_1 - \|(H_1)_{S_A}\|_1 + \|(H_1)_{S_A^C}\|_1 + \|XD\|_1 - \|(H_2)_{S_B}\|_1 + \|(H_2)_{S_B^C}\|_1, \end{aligned}$$

which gives  $\|(H_1)_{S_A^C}\|_1 + \|(H_2)_{S_B^C}\|_1 \leq \|(H_1)_{S_A}\|_1 + \|(H_2)_{S_B}\|_1$ , hence

$$\|H_1\|_1 + \|H_2\|_1 \leq 2(\|(H_1)_{S_A}\|_1 + \|(H_2)_{S_B}\|_1) \leq Cs\delta.$$

Here the last inequality is due to  $\|H_1\|_\infty = \|D^T D(D^{-1}(\hat{X} - X)D^{-T})D^T\|_\infty \leq 8\delta$ , similarly,  $\|H_2\|_\infty \leq 8\delta$ . Then we have the following constraints:

$$\|D^T(\hat{X} - X)\|_1 \leq Cs\delta, \quad \|D^{-1}(\hat{X} - X)\|_\infty \leq 2\delta.$$

Similar to the proof of Theorem 3.1, the inequalities above lead to

$$\|\hat{X} - X\|_F = \langle D^T(\hat{X} - X), D^{-1}(\hat{X} - X) \rangle^{\frac{1}{2}} \leq C\sqrt{s}\delta,$$

which is (3.3).  $\square$

### 3.3 Class 3: Reconstruction of Images Meeting the Minimum Separation Condition

In this section, we consider Class 3, where the image  $X$  satisfies Assumption 2.3. Same as in Class 1, we use  $Q_{col}$  (column by column quantization) for encoding. The reason why we do not use  $Q_{2D}$  is that the 2D minimum separation condition is not realistic on natural images.

For  $\underline{x} \in \mathbb{R}^N$ , its Sigma Delta quantization  $\underline{q} = Q^{\Sigma\Delta,\beta}(\underline{x})$ ,  $\beta = 1$  or  $2$ ,  $r \geq \beta$ . Again, use  $x$  and  $q$  instead of  $\underline{x}$  and  $\underline{q}$  for simplicity. Then (2.7) reduces to

$$\hat{x} = \arg \min_z \|D_1^\beta z\|_1 \text{ subject to } \|D^{-r}(z - q)\|_\infty \leq \delta/2, \quad \|(D^{-r}(z - q))_{N-r:N-1}\|_\infty < \left(\frac{1}{2N}\right)^r \delta. \quad (3.4)$$

There are two differences between this decoder and that for Class 1. 1) here  $D_1$  is the circulant difference matrix instead of the forward difference matrix. This is to ensure that the separation condition is satisfied at the boundary. 2) In order for the extra separation assumption to improve the error bound over Class 1, we need to use a few more bits to encode the boundary pixels. The total number of boundary bits is of order  $O(\log N)$ , which is negligible comparing to the  $O(N)$  bits needed for the interior pixels.

**Theorem 3.5.** *For high order  $\Sigma\Delta$  quantization, i.e.,  $r \geq 2$ , assume  $D_1^\beta x$  satisfies the  $\Lambda_M$ -minimization separation condition, and  $\hat{x}$  is a solution to (3.4), then for arbitrary resolution  $L \leq N/2$ , the following error bound holds:*

$$\|P_L(\hat{x} - x)\|_\infty \leq C \frac{L^2}{N^r} M^{r+\beta-2} \delta. \quad (3.5)$$

Here  $P_L$  is the projection onto the low frequency range with bandwidth  $2L$ , i.e.,  $P_L = F_L^* F_L$  with  $F_L$  being the first  $L$  rows of DFT matrix.

**Remark 3.6.** After applying the decoder (3.4) to each column, we put the reconstructed columns together to obtain the reconstructed image  $\hat{X}$ , the overall error bound in  $\ell_\infty$ -norm is then

$$\|P_L(\hat{X} - X)\|_\infty \leq C \frac{L^2}{N^r} M^{r+\beta-2} \delta.$$

Substituting  $L$  with  $N/2$ , we obtain

$$\|\hat{X} - X\|_F \leq C \frac{M^{r+\beta-2}}{N^{r-3}} \delta.$$

**Remark 3.7.** We consider using decoder (3.4) only for the columns satisfying the minimum separation condition. For these columns, Theorem 3.5 says that the worst case  $\ell_\infty$ -norm error bound for arbitrary resolution approaches 0 as  $N \rightarrow \infty$ .

### 3.3.1 Proof of Theorem 3.5

In order to prove Theorem 3.5, we perform the super-resolution analysis [9, 10, 31] under the Sigma Delta framework. We first need the following lemma.

**Lemma 3.8.** *For any feasible  $\tilde{x} \in \mathbb{R}^N$  which satisfies the constraints in (3.4), the following inequality holds:*

$$\|P_M D_1^\beta (\tilde{x} - x)\|_2 \lesssim \left( \frac{M}{N} \right)^{r+\beta} \sqrt{N} \delta.$$

*Proof.* Denote  $z = \tilde{x} - x$ , recall that for  $z \in \mathbb{R}^N$ , the discrete Fourier coefficient at frequency  $k$  is  $\mathcal{F}_k z = \sum_{n=0}^{N-1} z_n e^{-i2\pi \frac{kn}{N}}$ , we can see that  $P_M$  in the target inequality is equivalent to the sum of the outer products of  $\mathcal{F}_k$ ,  $k = 1, 2, \dots, M$ . For nonzero frequency  $k \neq 0$ , denote  $\alpha = \frac{1}{1 - e^{-i2\pi \frac{k}{N}}}$ , then we have

$$\mathcal{F}_k D_1 z = \sum_{n=0}^{N-1} (D_1 z)_n e^{-i2\pi \frac{kn}{N}} = (1 - e^{-i2\pi \frac{k}{N}}) \mathcal{F}_k z = \alpha^{-1} \mathcal{F}_k z.$$

Therefore  $\mathcal{F}_k D_1 z$  is equivalent to  $\mathcal{F}_k z$  multiplied by some constant depending on  $k$ . Next, we show that  $\mathcal{F}_k D^{-r} z$  is also close to a scaling of  $\mathcal{F}_k z$ , which further leads to the relationship between  $\mathcal{F}_k D_1^\beta z$  and  $\mathcal{F}_k D^{-r} z$ . Direct calculation gives

$$\begin{aligned}\mathcal{F}_k D^{-1} z &= \sum_{n=0}^{N-1} \left( \sum_{j=0}^n z_j \right) e^{-i2\pi \frac{kn}{N}} = \sum_{n=0}^{N-1} z_n \sum_{j=n}^{N-1} e^{-i2\pi \frac{kj}{N}} \\ &= \frac{1}{1 - e^{-i2\pi \frac{k}{N}}} \sum_{n=0}^{N-1} z_n (e^{-i2\pi \frac{kn}{N}} - 1) = \alpha \mathcal{F}_k z - \alpha (D^{-1} z)_{N-1}.\end{aligned}$$

Similarly,

$$\mathcal{F}_k D^{-2} z = \alpha \mathcal{F}_k D^{-1} z - \alpha (D^{-2} z)_{N-1} = \alpha^2 \mathcal{F}_k z - \alpha^2 (D^{-1} z)_{N-1} - \alpha (D^{-2} z)_{N-1},$$

$$\mathcal{F}_k D^{-3} z = \alpha^3 \mathcal{F}_k z - \alpha^3 (D^{-1} z)_{N-1} - \alpha^2 (D^{-2} z)_{N-1} - \alpha (D^{-3} z)_{N-1}.$$

More generally, for  $\beta = 1$  or  $2$ ,  $r \geq 2$ ,

$$\begin{aligned}\mathcal{F}_k D^{-r} z &= \alpha^r \mathcal{F}_k z - \alpha^r (D^{-1} z)_{N-1} - \alpha^{r-1} (D^{-2} z)_{N-1} - \cdots - \alpha (D^{-r} z)_{N-1} \\ &= \alpha^{r+\beta} \mathcal{F}_k D_1^\beta z - \alpha^r (D^{-1} z)_{N-1} - \alpha^{r-1} (D^{-2} z)_{N-1} - \cdots - \alpha (D^{-r} z)_{N-1}.\end{aligned}$$

Multiplying  $\alpha^{-(r+\beta)}$  on both sides and rearranging the terms gives,

$$\begin{aligned}\mathcal{F}_k D_1^\beta z &= (1 - e^{-i2\pi \frac{k}{N}})^{r+\beta} \mathcal{F}_k D^{-r} z + (1 - e^{-i2\pi \frac{k}{N}})^\beta (D^{-1} z)_{N-1} \\ &\quad + (1 - e^{-i2\pi \frac{k}{N}})^{\beta+1} (D^{-2} z)_{N-1} + \cdots + (1 - e^{-i2\pi \frac{k}{N}})^{\beta+r-1} (D^{-r} z)_{N-1}.\end{aligned}$$

Note that for  $k = 0$ ,  $\mathcal{F}_0 D_1^\beta z = \sum_{n=0}^{N-1} (D_1^\beta z)_n = 0$ . Then the equation above holds for all integer  $k$  with  $0 \leq |k| \leq N/2$ . Denote  $\Lambda \in \mathbb{C}^{2M+1, 2M+1}$  as the diagonal matrix with diagonal entries being  $1 - e^{-i2\pi \frac{k}{N}}$ ,  $-M \leq k \leq M$ , we obtain the matrix form of the previous equation

$$\begin{aligned}F_M D_1^\beta z &= \Lambda^{r+\beta} F_M D^{-r} z + \Lambda^\beta (D^{-1} z)_{N-1} \mathbf{1} + \Lambda^{\beta+1} (D^{-2} z)_{N-1} \mathbf{1} + \cdots + \Lambda^{\beta+r-1} (D^{-r} z)_{N-1} \mathbf{1} \\ &= \Lambda^{r+\beta} F_M D^{-r} z + \sum_{\ell=1}^r \Lambda^{\beta+\ell-1} (D^{-\ell} z)_{N-1}.\end{aligned}$$

Recall that  $F_M$  contains the rows of DFT matrix with frequencies in  $\{-L, -L+1, \dots, L\}$ . Multiplying  $\frac{1}{N} F_M^*$  on both sides of the above equation and replace  $z$  with  $z = \tilde{x} - x$ , we have

$$P_M D_1^\beta (\tilde{x} - x) = \frac{1}{N} F_M^* \Lambda^{r+\beta} F_M D^{-r} (\tilde{x} - x) + \sum_{\ell=1}^r \frac{1}{N} F_M^* \Lambda^{\beta+\ell-1} (D^{-\ell} (\tilde{x} - x))_{N-1}.$$

Note that  $\left|1 - e^{-i2\pi \frac{k}{N}}\right| \leq 2\pi \frac{|k|}{N} \leq 2\pi \frac{M}{N}$ , hence  $\left\| \frac{1}{N} F_M^* \Lambda^\ell \right\|_2 \lesssim \frac{1}{\sqrt{N}} \left( \frac{M}{N} \right)^\ell$ , and the following error bound in  $\ell_2$  norm holds

$$\begin{aligned} \|P_M D_1^\beta (\tilde{x} - x)\|_2 &\leq \left\| \frac{1}{N} F_M^* \Lambda^{r+\beta} F_M \right\|_2 \|D^{-r}(\tilde{x} - x)\|_2 + \sum_{\ell=1}^r \left\| \frac{1}{N} F_M^* \Lambda^{\beta+\ell-1} \right\|_2 \sqrt{M} |D^{-\ell}(\tilde{x} - x)_{N-1}| \\ &\lesssim \left( \frac{M}{N} \right)^{r+\beta} \sqrt{N} \delta + \sum_{\ell=1}^r \left( \frac{M}{N} \right)^{\beta+\ell-\frac{1}{2}} \cdot 2^r \left( \frac{1}{2N} \right)^r \delta \\ &\lesssim \left( \frac{M}{N} \right)^{r+\beta} \sqrt{N} \delta. \end{aligned} \quad (3.6)$$

Here (3.6) is due to the feasibility of  $\tilde{x}$  and the true signal  $x$ :  $\|(D^{-r}(\tilde{x} - q))_{N-r:N-1}\|_\infty < \left( \frac{1}{2N} \right)^r \delta$  and  $\|(D^{-r}(x - q))_{N-r:N-1}\|_\infty < \left( \frac{1}{2N} \right)^r \delta$ . These two inequalities and the triangle inequality imply  $\|(D^{-r}(\tilde{x} - x))_{N-r:N-1}\|_\infty < 2 \left( \frac{1}{2N} \right)^r \delta$ . From this last inequality, we further have for all  $1 \leq \ell \leq r$ ,  $|D^{-\ell}(\tilde{x} - x)_{N-1}| \leq 2^r \left( \frac{1}{2N} \right)^r \delta$ , which leads to (3.6).  $\square$

Substituting  $\tilde{x}$  by  $\hat{x}$  in Lemma 3.8, we can see the low frequency error  $P_M D_1^\beta (\hat{x} - x)$  decreases with the  $\Sigma\Delta$  quantization order  $r$ . Denote  $h = D_1^\beta (\hat{x} - x)$ , we will divide  $h$  into two parts based on whether the location of each entry is within a neighbor of some nonzero element of  $D_1^\beta x$ .

For simplicity of proof, we view the vectors  $x, \hat{x}, h \in \mathbb{R}^N$  as signals on  $[0, 1]$  sampled at grid  $t_n = n/N, n = 0, 1, \dots, N-1$ . For  $D_1^\beta x$  satisfying the  $\Lambda_M$ -minimum separation condition with support set  $S = \{\xi_1, \xi_2, \dots, \xi_s\} \subset [0, 1]$ , as in [31], we define

$$S_M(j) = \{x \in [0, 1] : |x - \xi_j| \leq 0.16M^{-1}\}, \quad j = 1, 2, \dots, s,$$

and

$$S_M = \bigcup_{j=1}^s S_M(j), \quad S_M^c = [0, 1] \setminus S_M.$$

Then the following lemma holds.

**Lemma 3.9.** [Discrete version of Proposition 2.3, [31]] If  $D_1^\beta x$  satisfies the  $\Lambda_M$ -minimum separation condition, with the  $S_M$  defined above, there exists a constant  $C > 0$  such that the following hold

$$\sum_{t_n \in S_M^c} |h_n| \leq C \sqrt{N} \|P_M h\|_2, \quad (3.7)$$

$$\sum_j \sum_{t_n \in S_M(j)} |h_n| |t_n - s_j|^2 \leq C M^{-2} \sqrt{N} \|P_M h\|_2. \quad (3.8)$$

*Proof.* Denote the restriction of  $h$  to a set  $S$  as  $P_S h$ , and  $P_S h(\xi_j) = |P_S h(\xi_j)| e^{i\phi_j}$ ,  $j = 1, 2, \dots, s$ . By Lemma 6.1 in the appendix, take  $v_j = e^{i\phi_j}$ ,  $j = 1, 2, \dots, s$ , there exist  $f(t) = \sum_{k=-M}^M c_k e^{i2\pi kt}$  defined on  $[0, 1]$  and constants  $C_1, C_2$  such that

$$f(t_j) = e^{i\phi_j}, \quad j = 1, 2, \dots, s, \quad (3.9)$$

$$|f(t)| \leq 1 - C_1 M^2 (t - \xi_j)^2, \quad t \in S_M(j), \quad (3.10)$$

$$|f(t)| < 1 - C_2, \quad t \in S_M^c. \quad (3.11)$$

Denote  $f_n = f(t_n)$  where  $t_n = n/N$ ,  $n = 0, 1, \dots, N-1$ , then

$$\begin{aligned} \sum_{t_n \in S} |h_n| &= \left| \sum_{t_n \in S} \bar{f}_n h_n \right| \\ &\leq \left| \sum_{n=0}^{N-1} \bar{f}_n h_n \right| + \left| \sum_{t_n \in S_M^c} \bar{f}_n h_n \right| + \left| \sum_j \sum_{t_n \in S_M(j) \setminus \{s_j\}} \bar{f}_n h_n \right| \\ &\leq \left| \sum_{n=0}^{N-1} \bar{f}_n h_n \right| + (1 - C_2) \sum_{t_n \in S_M^c} |h_n| + \sum_j \sum_{t_n \in S_M(j)} (1 - C_1 M^2 (t_n - \xi_j)^2) |h_n| \\ &= \left| \sum_{n=0}^{N-1} \bar{f}_n h_n \right| + \sum_{t_n \in S^c} |h_n| - C_2 \sum_{t_n \in S_M^c} |h_n| - C_1 M^2 \sum_j \sum_{t_n \in S_M(j)} (t_n - \xi_j)^2 |h_n|. \end{aligned}$$

Rearrange the inequality, we obtain

$$C_2 \sum_{t_n \in S_M^c} |h_n| + C_1 M^2 \sum_j \sum_{t_n \in S_M(j)} (t_n - \xi_j)^2 |h_n| \leq \left| \sum_{n=0}^{N-1} \bar{f}_n h_n \right| + \sum_{t_n \in S^c} |h_n| - \sum_{t_n \in S} |h_n|. \quad (3.12)$$

Note that  $\left| \sum_{n=0}^{N-1} \bar{f}_n h_n \right| = |\langle f, h \rangle| = |\langle f, P_M h \rangle| \leq \|f\|_2 \|P_M h\|_2 \leq \sqrt{N} \|P_M h\|_2$ , also note that  $\hat{x}$  is a solution to (3.4), so we have

$$\|D_1^\beta x\|_1 \geq \|D_1^\beta \hat{x}\|_1 = \|D_1^\beta x + h\|_1 \geq \sum_{t_n \in S} |(D_1^\beta x)_n| - \sum_{t_n \in S} |h_n| + \sum_{t_n \in S^c} |h_n|.$$

Rearranging the above inequality, we have

$$\sum_{t_n \in S^c} |h_n| - \sum_{t_n \in S} |h_n| \leq 0.$$

Then (3.12) becomes

$$C_2 \sum_{t_n \in S_M^c} |h_n| + C_1 M^2 \sum_j \sum_{t_n \in S_M(j)} (t_n - \xi_j)^2 |h_n| \leq \sqrt{N} \|P_M h\|_2.$$

From this inequality we can derive (3.7) and (3.8).  $\square$

*Proof of Theorem 3.5.* The proof contains two steps, in the first step, we bound  $\|K * D_1^\beta(\hat{x} - x)\|_\infty$  for arbitrary kernel  $K$  with period 1. In the second step, we pick a special kernel to prove the theorem.

For an arbitrary  $x_0 \in \left\{0, \frac{1}{N}, \dots, \frac{N-1}{N}\right\}$ ,

$$|K * h(x_0)| = \left| \sum_{n=0}^{N-1} K(x_0 - t_n) h_n \right| \leq \left| \sum_j \sum_{t_n \in S_M(j)} K(x_0 - t_n) h_n \right| + \|K\|_\infty \sum_{t_n \in S_M^c} |h_n|. \quad (3.13)$$

On the interval  $S_M(j)$ , approximate  $K(x_0 - t_n)$  with its first-order Taylor expansion around  $x_0 - \xi_j$ ,

$$K(x_0 - t_n) = K(x_0 - \xi_j) + K'(x_0 - \xi_j)(\xi_j - t_n) + \frac{1}{2}K''(\mu_n)|t_n - \xi_j|^2, \quad x \in S_M(j),$$

with some  $\mu_n \in S_M(j)$  depending on  $x_0, s_j, x$ . Inserting this in to (3.13), we obtain

$$\begin{aligned} |K * h(x_0)| &\leq \left| \sum_j \sum_{t_n \in S_M(j)} (K(x_0 - \xi_j) - K'(x_0 - \xi_j)(t_n - \xi_j)) h_n \right| \\ &\quad + \frac{1}{2} \|K''\|_\infty \sum_j \sum_{t_n \in S_M^c} |t_n - \xi_j|^2 |h_n| + \|K\|_\infty \sum_{t_n \in S_M^c} |h_n|. \end{aligned}$$

To bound the first term on the right hand side, we use an interpolation argument. Let  $a, b \in \mathbb{C}^s$  such that  $a_j = K(x_0 - \xi_j)$ ,  $b_j = -K'(x_0 - \xi_j)$  and by Proposition 2.4 in [31], there exists a function  $f \in C([0, 1], \Lambda_M)$  such that

$$\|f\|_\infty \lesssim \|K\|_\infty + M^{-1} \|K'\|_\infty,$$

$$|f(x) - a_j - b_j(x - \xi_j)| \lesssim (M^2 \|K\|_\infty + M \|K'\|_\infty) |x - \xi_j|^2, \quad x \in S_M(j),$$

which gives

$$\begin{aligned} &\left| \sum_j \sum_{t_n \in S_M(j)} (K(x_0 - \xi_j) - K'(x_0 - \xi_j)(t_n - \xi_j)) h_n \right| \\ &\leq \left| \sum_j \sum_{t_n \in S_M(j)} (f(t_n) - K(x_0 - \xi_j) + K'(x_0 - \xi_j)(t_n - \xi_j)) h_n \right| + \left| \sum_{t_n \in S_M} f_n h_n \right| \\ &\lesssim (M^2 \|K\|_\infty + M \|K'\|_\infty) \sum_j \sum_{t_n \in S_M(j)} |t_n - \xi_j|^2 |h_n| + \left| \sum_{n=0}^{N-1} f_n h_n \right| + \left| \sum_{n \in S_M^c} f_n h_n \right|. \end{aligned}$$

Also, we obtain

$$\left| \sum_{t_n \in S_M^c} f_n h_n \right| \lesssim (\|K\|_\infty + M^{-1} \|K'\|_\infty) \sum_{t_n \in S_M^c} |h_n|,$$

$$\left| \sum_{n=0}^{N-1} f_n h_n \right| \leq \|f\|_2 \|P_M h\|_2 \lesssim (\|K\|_\infty + M^{-1} \|K'\|_\infty) \sqrt{N} \|P_M h\|_2.$$

Combining these results, we obtain

$$\begin{aligned} |K * h(x_0)| &\lesssim (2\|K\|_\infty + M^{-1} \|K'\|_\infty) \sum_{t_n \in S_M^c} |h_n| \\ &\quad + (\|K\|_\infty + M^{-1} \|K'\|_\infty) \sqrt{N} \|P_M h\|_2 \\ &\quad + (M^2 \|K\|_\infty + M \|K'\|_\infty + \|K''\|_\infty) \sum_j \sum_{t_n \in S_M(j)} |t_n - \xi_j|^2 |h_n| \\ &\lesssim (\|K\|_\infty + M^{-1} \|K'\|_\infty + M^{-2} \|K''\|_\infty) \sqrt{N} \|P_M h\|_2. \end{aligned} \tag{3.14}$$

Next, for arbitrary resolution  $L$ , denote  $K_L(x) = \frac{1}{N} \sum_{k=-L, k \neq 0}^L e^{i2\pi kx}$ , then by direct calculation we obtain

$$P_L(\hat{x} - x) = K_L * (\hat{x} - x) + \frac{1}{N} \sum_{n=0}^{N-1} (\hat{x} - x)_n \mathbf{1}.$$

We will bound the two terms on the RHS separately, the second term is easy to bound due to the boundary constraint in (3.4) which forces the absolute value of the last  $r$  rows in  $D^{-r}(\hat{x} - x)$  to be smaller than  $2 \cdot (\frac{1}{2N})^r$ , then

$$\left| \sum_{n=0}^{N-1} (\hat{x} - x)_n \right| = |(D^{-1}(\hat{x} - x))_{N-1}| = 2^{r-1} \|D^{-r}(\hat{x} - x)_{N-r:N-1}\|_\infty \leq \left(\frac{1}{N}\right)^r.$$

This gives  $\|P_L(\hat{x} - x) - K_L * (\hat{x} - x)\|_\infty < \frac{1}{N^r}$ . Next, we derive an upper bound on the first term  $\|K_L * (\hat{x} - x)\|_\infty$ .

Case I: TV order= 1:

For  $K_L(x)$ , we construct an auxiliary function

$$\tilde{K}_L(x) = \frac{1}{N} \sum_{k=-L, k \neq 0}^L \frac{1 - e^{i2\pi k(x + \frac{1}{N})}}{1 - e^{i2\pi \frac{k}{N}}}, \quad x \in [0, 1].$$

Notice that

$$\tilde{K}_L(t_j) = \frac{1}{N} \sum_{k=-L, k \neq 0}^L \frac{1 - e^{i2\pi k \frac{j+1}{N}}}{1 - e^{i2\pi \frac{k}{N}}} = \frac{1}{N} \sum_{k=-L, k \neq 0}^L \sum_{n=0}^j e^{i2\pi k \frac{n}{N}} = \sum_{n=0}^j K_L(t_n), \quad j = 0, 1, \dots, N-1.$$

Hence  $\tilde{K}_L$  satisfies the property

$$D_1 \tilde{K}_L(t_j) = \tilde{K}_L(t_j) - \tilde{K}_L(t_{j-1}) = K_L(t_j), \quad \forall j = 1, 2, \dots, N-1.$$

Also, since  $\tilde{K}_L(t_{N-1}) = 0$ , we have  $D_1 \tilde{K}_L(t_j) = K_L(t_j)$ ,  $\forall j = 0, 1, \dots, N-1$ . Then the bound  $\|K_L * (\hat{x} - x)\|_\infty$  is equivalent to

$$\|K_L * (\hat{x} - x)\|_\infty = \|D_1 \tilde{K}_L * (\hat{x} - x)\|_\infty = \|\tilde{K}_L * D_1(\hat{x} - x)\|_\infty = \|\tilde{K}_L * h\|_\infty.$$

Now we show that the infinity norm of  $\tilde{K}_L(x)$  is bounded by some constant for arbitrary  $L \leq N/2$  and  $x \in [0, 1]$ , then we can bound  $\|\tilde{K}_L * h\|$  by (3.14). Since  $e^{i2\pi kx}$  is 1-periodic, we have

$$\begin{aligned} \sup_x |\tilde{K}_L(x)| &= \frac{1}{N} \sup_x \left| \sum_{k=-L, k \neq 0}^L \frac{1 - e^{i2\pi kx}}{1 - e^{i2\pi \frac{k}{N}}} \right| \\ &= \frac{1}{N} \sup_x \left| \sum_{k=1}^L \frac{1 - \cos(2\pi kx) - i \sin(2\pi kx)}{1 - \cos(2\pi \frac{k}{N}) - i \sin(2\pi \frac{k}{N})} + \frac{1 - \cos(2\pi kx) + i \sin(2\pi kx)}{1 - \cos(2\pi \frac{k}{N}) + i \sin(2\pi \frac{k}{N})} \right| \\ &= \frac{1}{N} \sup_x \left| \sum_{k=1}^L \frac{(1 - \cos(2\pi kx))(1 - \cos(2\pi \frac{k}{N})) + \sin(2\pi kx) \sin(2\pi \frac{k}{N})}{1 - \cos(2\pi \frac{k}{N})} \right| \\ &= \frac{1}{N} \sup_x \left| \sum_{k=1}^L (1 - \cos(2\pi kx)) + \frac{\sin(2\pi kx) \cos(\pi \frac{k}{N})}{\sin(\pi \frac{k}{N})} \right| \\ &\leq \frac{L}{N} + \frac{1}{N} \sup_x \left| \sum_{k=1}^L \frac{\sin(2\pi kx) \cos(\pi \frac{k}{N}) - \sin(\pi \frac{k}{N}) \cos(2\pi kx)}{\sin(\pi \frac{k}{N})} \right| \\ &= \frac{L}{N} + \frac{1}{N} \sup_x \left| \sum_{k=1}^L \frac{\sin(2\pi k(x - \frac{1}{2N}))}{\sin(\pi \frac{k}{N})} \right| \\ &= \frac{L}{N} + \frac{1}{N} \sup_x \left| \sum_{k=1}^L \frac{\sin(2\pi kx)}{\sin(\pi \frac{k}{N})} \right|. \end{aligned}$$

Notice that for  $k \leq L \leq N/2$ ,  $\pi \frac{k}{N} \leq \frac{\pi}{2}$ , then  $\sin(\pi \frac{k}{N})$  is of the same order as  $\pi \frac{k}{N}$  since for all  $0 < x \leq \frac{\pi}{2}$ ,  $x - \frac{x^3}{6} \leq \sin(x) < x$ , which further gives  $0.58\pi \frac{k}{N} \leq \pi \frac{k}{N} - (\pi \frac{k}{N})^3/6 \leq \sin(\pi \frac{k}{N}) < \pi \frac{k}{N}$ . Then we can see that

$$\begin{aligned} \left| \frac{1}{N} \sum_{k=1}^L \frac{\sin(2\pi kx)}{\sin(\pi \frac{k}{N})} - \sum_{k=1}^L \frac{\sin(2\pi kx)}{\pi k} \right| &= \frac{1}{N} \left| \sum_{k=1}^L \sin(2\pi kx) \left( \frac{1}{\sin(\pi \frac{k}{N})} - \frac{1}{\pi \frac{k}{N}} \right) \right| \\ &= \frac{1}{N} \left| \sum_{k=1}^L \sin(2\pi kx) \frac{\pi \frac{k}{N} - \sin(\pi \frac{k}{N})}{\sin(\pi \frac{k}{N}) \pi \frac{k}{N}} \right| \\ &\leq \frac{1}{N} \sum_{k=1}^L \frac{\frac{1}{6} (\pi \frac{k}{N})^3}{0.58 (\pi \frac{k}{N})^2} \\ &\leq 0.23. \end{aligned}$$

It is known that for arbitrary  $n \in \mathbb{N}$  and  $x \in \mathbb{R}$ , the summation  $\left| \sum_{k=1}^n \frac{\sin(2\pi kx)}{k} \right|$  is uniformly bounded by some constant smaller than 2 ([1]). Hence  $\tilde{K}_L(x)$  is also bounded, there exists some constant  $C$  such that  $\|\tilde{K}_L\|_\infty \leq C$ . Therefore by (3.14) we have,

$$\|K_L * (\hat{x} - x)\|_\infty \leq \|D_1 \tilde{K}_L * (\hat{x} - x)\|_\infty = \|\tilde{K}_L * h\|_\infty \leq C \frac{L^2}{M^2} \sqrt{N} \cdot \frac{M^{r+1}}{N^{r+\frac{1}{2}}} \delta = C \frac{L^2}{N} \left(\frac{M}{N}\right)^{r-1} \delta.$$

For the last inequality, we used Bernstein's inequality for trigonometric sums [4] to obtain  $\|\tilde{K}_L\|_\infty \leq C$ ,  $\|\tilde{K}'_L\|_\infty \leq CL$ ,  $\|\tilde{K}''_L\|_\infty \leq CL^2$ .

Case II: TV order=2:

Consider  $\tilde{K}_L(x) = -\frac{1}{N} \sum_{k=-L, k \neq 0}^L \frac{e^{i2\pi \frac{k}{N}} - e^{i2\pi k(\frac{2}{N}+x)}}{(1 - e^{i2\pi \frac{k}{N}})^2}$ . Similar to Case I, we can show  $D_1^2 \tilde{K}_L(t_j) = K_L(t_j)$ ,  $\forall j = 0, 1, \dots, N-1$ , and  $\|\tilde{K}\|_\infty \leq N$ . Then

$$\|K_L * (\hat{x} - x)\|_\infty \leq \|D_1^2 \tilde{K}_L * (\hat{x} - x)\|_\infty = \|\tilde{K}_L * h\|_\infty \leq C \frac{L^2}{M^2} N^{\frac{3}{2}} \cdot \frac{M^{r+2}}{N^{r+\frac{3}{2}}} \delta = CL^2 \left(\frac{M}{N}\right)^r \delta.$$

In conclusion, for  $\beta = 1$  or  $2$ , we have the  $\ell_\infty$ -norm error bound

$$\|K_L * (\hat{x} - x)\|_\infty \leq C \frac{L^2}{N^r} M^{r+\beta-2} \delta,$$

which further gives

$$\|P_L(\hat{x} - x)\|_\infty \leq \|K_L * (\hat{x} - x)\|_\infty + \left\| \frac{1}{N} \sum_{n=0}^{N-1} (\hat{x} - x)_n \mathbf{1} \right\|_\infty \leq C \frac{L^2}{N^r} M^{r+\beta-2} \delta.$$

□

## 4 Optimization

In this section, we discuss the optimization algorithm for solving (3.1). Since all optimization problems proposed in this paper can be solved in similar ways, we only discuss the simplest case when the TV order  $\beta$  and the quantization order  $r$  are both 1, which reduces (3.1) to

$$\min_z \|D^T z\|_1 \quad \text{subject to } \|D^{-1}(z - q)\|_\infty \leq \delta/2. \quad (4.1)$$

Let us start with writing out the Lagrangian dual of (4.1)

$$\mathcal{L}(z, y) = \|D^T z\|_1 - \frac{\delta}{2} \|y\|_1 + \langle y, D^{-1}(z - q) \rangle. \quad (4.2)$$

This dual formulation (4.2) is a special case of the general form

$$\max_y \min_x \langle Lx, y \rangle + g(x) - f^*(y), \quad (4.3)$$

which is known to be solvable by primal-dual algorithms such as the Chambolle-Pock method (Algorithm 1).

---

**Algorithm 1:** Solve (4.3) using Chambolle-Pock Method

---

**Initializations:**  $\tau, \sigma > 0, \tau\sigma < 1, \theta \in [0, 1], x_0, y_0$ . and set  $\bar{x}_0 = x_0$

**Iterations:** Update  $x_n, y_n, \bar{x}_n$  as follows:

$$\begin{cases} y_{n+1} = \text{Prox}_{\sigma f^*}(y_n + \sigma L \bar{x}_n) & (a) \\ x_{n+1} = \text{Prox}_{\tau g}(x_n - \tau L^* y_{n+1}) & (b) \\ \bar{x}_{n+1} = x_{n+1} + \theta(x_{n+1} - x_n) & (c) \end{cases}$$


---

Comparing corresponding terms in (4.3) and (4.2), one naturally recognizes  $x = D^T z$ ,  $L = D^{-1} D^{-T}$ ,  $g(x) = \|x\|_1$ ,  $f^*(y) = \frac{\delta}{2} \|y\|_1$ , then

$$\mathcal{L}(x, y) = \|x\|_1 - \frac{\delta}{2} \|y\|_1 + \langle y, D^{-1} D^{-T} x - D^{-1} q \rangle \equiv \langle Lx, y \rangle + g(x) - f^*(y). \quad (4.4)$$

However, applying Algorithm 1 to this  $\mathcal{L}(x, y)$  results in a very slow convergence, since  $L$  has a poor condition number (of order  $O(N^2)$ ).

A more efficient way is to move the large condition number to the sub-problem (b) via a change of variable  $x = D^{-1}(z - q)$ , or  $z = Dx + q$ . In this way, the large condition number of  $L$  is moved to the  $g$  in the sub-problem (b) in (4.3). The large condition number in  $g$  is harmless to the inner loop due to the use of the proximal map. After this change of variable, the primal-dual objective becomes

$$\mathcal{L}(x, y) = \langle y, x \rangle + \|D^T D x + D^T q\|_1 - \frac{\delta}{2} \|y\|_1. \quad (4.5)$$

Next, let  $g(x) = \|D^T D x + D^T q\|_1$ ,  $f^*(y) = \frac{\delta}{2} \|y\|_1$ , we can see that (4.5) also fits into the form of (4.3). Applying Chambolle-Pock Method to solving (4.5), it gives the following

algorithm

---

**Algorithm 2:** Solve (4.5) using Chambolle-Pock Method

---

**Initializations:**  $\tau, \sigma > 0, \tau\sigma < 1, \theta \in [0, 1], x_0, y_0$ . and set  $\bar{x}_0 = x_0$

**Iterations:** Update  $x_n, y_n, \bar{x}_n$  as follows:

$$\begin{cases} y_{n+1} = \arg \min_y \frac{\sigma\delta}{2} \|y\|_1 + \frac{1}{2} \|y - (y_n + \sigma\bar{x}_n)\|^2 & (a) \\ x_{n+1} = \tau \|D^T D x + D^T q\|_1 + \frac{1}{2} \|x - (x_n - \tau y_{n+1})\|^2 & (b) \\ \bar{x}_{n+1} = x_{n+1} + \theta(x_{n+1} - x_n) & (c) \end{cases}$$

---

Note that it has been shown in [11] that when  $L = I$  ( $I$  is the identity matrix), step sizes  $\tau = 1/\sigma$  and extrapolation rate  $\theta$  is set to 1, PDHG is equivalent to DRS and ADMM. Hence the above algorithm can also be derived by appropriate applications of the ADMM algorithm when those special step sizes are used.

In Algorithm 2, step (a) has a closed form solution. To solve (b), we apply ADMM algorithm (see, e.g., [8]), the procedure of which is stated in Algorithm 3.

---

**Algorithm 3:** Solve (b) in Algorithm 2 by ADMM

---

**Initializations:**  $\rho > 0, x_0, u_0, b_0$

**Iterations:** Update  $x_n, u_n, b_n$  as follows:

$$\begin{cases} x_{n+1} = \arg \min_x \frac{1}{2} \|x - (x_n - \tau y_{n+1})\|_2^2 + \frac{\rho}{2} \|D^T D x + D^T q - u_n + b_n\|_2^2 \\ u_{n+1} = \arg \min_u \tau \|u\|_1 + \frac{\rho}{2} \|D^T D x_{n+1} + D^T q - u + b_n\|_2^2 \\ b_{n+1} = b_n + D^T D x_{n+1} + D^T q - u_{n+1} \end{cases}$$

---

## 5 Numerical simulation

In this section, we show the numerical performance of the proposed decoder on both 1D synthetic signals and natural images.

### 5.1 1D synthetic signal

We design an experiment to confirm the benefits of the proposed methods over MSQ on 1D signals (representing columns of images) proved in Theorem 3.1. The signal to be quantized is piece-wise constant or piece-wise linear with random boundary locations and random height/slope on each piece, which satisfies our assumption 2.1. We compare MSQ with Sigma Delta quantization coupled with the decoder (3.1). The result is displayed in Figure 4. We see from (a) that, with the same number of bits, the reconstructed signal using 1<sup>st</sup>

order  $\Sigma\Delta$  quantization and decoder (3.1) is closer to the true signal and generally preserves the piece-wise constant structure. (b) shows that the piece-wise linear signal is also better reconstructed by the proposed method. As real images never strictly satisfy our small  $\ell_0$  norm assumption, in (c), we test the stability of our method by adding random noises to the clean piece-wise constant or linear signals. We see that the proposed encoder-decoder pair is pretty robust in maintaining its superior performance over MSQ on signals slightly violating our model assumption.

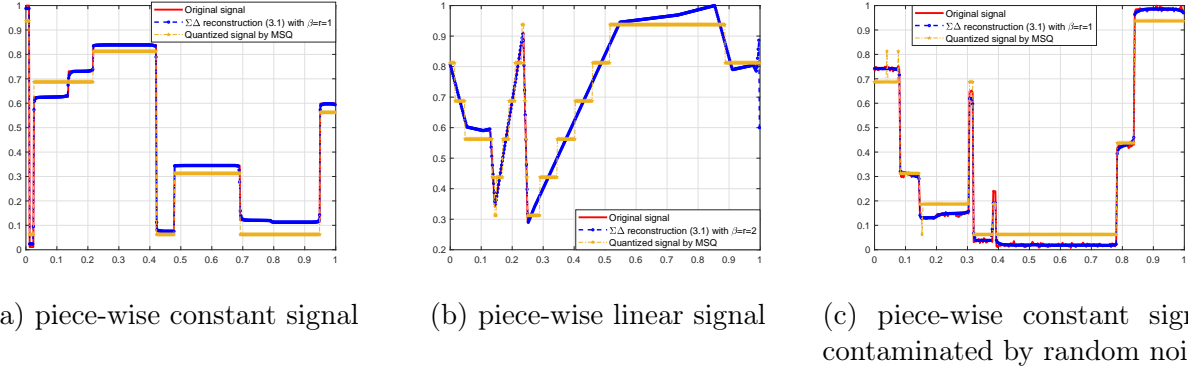


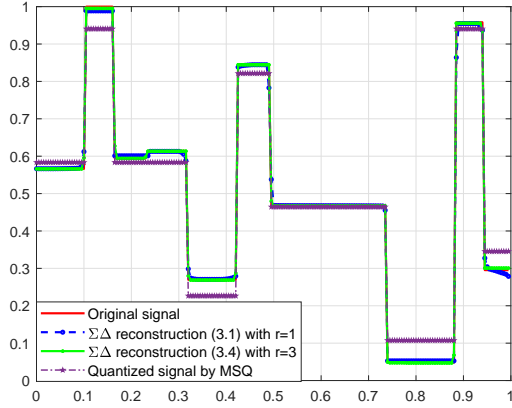
Figure 4: A comparison of various 1D signal reconstruction results between the proposed encoder-decoder pairs and MSQ. (a): the signal is piece-wise constant, not satisfying the minimum separation condition, we compare MSQ with 1<sup>st</sup> order  $\Sigma\Delta$  quantization. The decoder used for reconstruction is (3.1) with  $\beta = 1$ . The SNR of the reconstructed image from  $\Sigma\Delta$  quantization is 37.00, and the SNR of MSQ is 21.95. (b): the signal is piece-wise linear, we used 2<sup>nd</sup> order  $\Sigma\Delta$  quantization and decoder (3.1) with  $\beta = 2$ , the SNR of the  $\Sigma\Delta$  reconstruction is 37.30, and the SNR of MSQ is 27.33. (c): the signal is piece-wise constant with random noise, we use 1<sup>st</sup> order  $\Sigma\Delta$  quantization and decoder (3.1) with  $\beta = 1$ , SNR of  $\Sigma\Delta$  reconstruction is 33.40, and SNR of MSQ is 20.93.

As analyzed in Section 3.3, if the minimum separation condition is met, the quantization error can be further reduced by using high order  $\Sigma\Delta$  quantization. In both (a) and (b) of Figure 5, the reconstructed signals from a higher order of  $\Sigma\Delta$  quantization are closer to the true signal than those from a lower order of quantization order, confirming our theoretical result in Theorem 3.5.

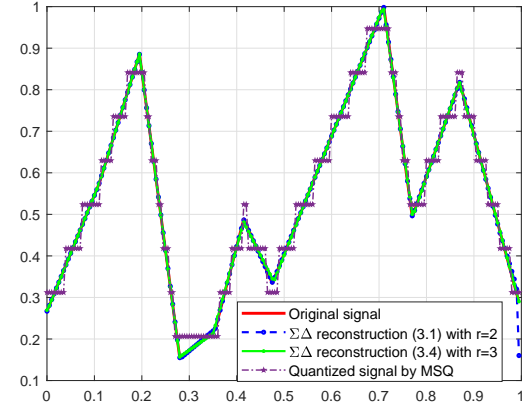
## 5.2 2D natural images

In this section, we present numerical results on natural images. We observe that the best performances are usually achieved when the TV order and the  $\Sigma\Delta$  quantization order are both set to 1, perhaps because the test images fit our Class 2 model better.

In the first example, we compare on gray-scale images, the results of 2D Sigma Delta quantization  $Q_{2D}$  coupled with decoder (2.6) (sd2D), 1D Sigma Delta quantization  $Q_{col}$  coupled with decoder (2.5) (sd1D) and the MSQ quantization, all quantization used the



(a) piece-wise constant signal



(b) piece-wise linear signal

Figure 5: Reconstruction result of signals that satisfy minimum separation condition. (a) the signal is piece-wise constant. For  $\Sigma\Delta$  quantization, we use 1<sup>st</sup> order  $\Sigma\Delta$  quantization and decoder (3.1) with  $\beta = r = 1$ ; 3<sup>rd</sup> order  $\Sigma\Delta$  quantization and decoder (3.4) with  $\beta = 1, r = 3$ . The SNR of the reconstructed signals are 33.69 and 41.90, respectively. The SNR of MSQ is 24.13. (b) the signal is piece-wise linear, for  $\Sigma\Delta$  quantization, we use 2<sup>nd</sup> order  $\Sigma\Delta$  quantization and decoder (3.1) with  $\beta = r = 2$ ; 3<sup>rd</sup> order  $\Sigma\Delta$  quantization and decoder (3.4) with  $\beta = 2, r = 3$ . The SNR of the reconstructed signals are 36.11 and 47.02, respectively. The SNR of MSQ is 25.70.

same number of bits and the optimal alphabets. In Figure 6, we see that in terms of visual quality, (sd2D) is better than (sd1D) and much better than MSQ. In terms of the PSNR, (sd1D) is slightly better than (sd2D) and better than MSQ.

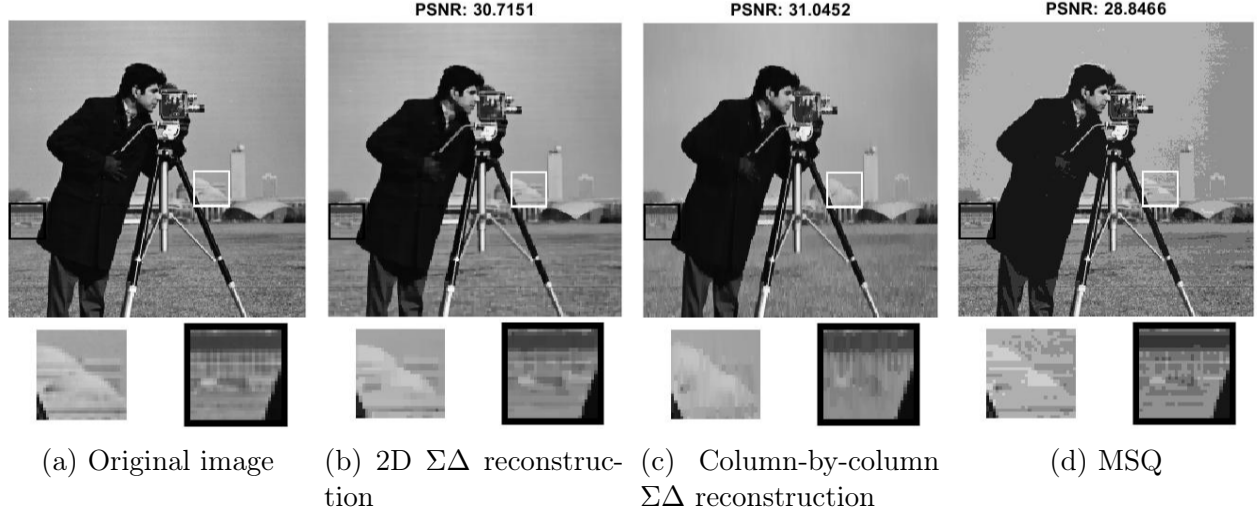


Figure 6: Cameraman reconstruction results, here we used 3-bit quantization in both  $\Sigma\Delta$  and MSQ cases. (a) is the ground truth. (b) the image is quantized by  $Q_{2D}$  and the decoder is (2.6). (c) both quantization and reconstruction is carried out column-by-column, we use 1<sup>st</sup> order  $\Sigma\Delta$  quantization and decoder (2.5). (d) MSQ quantization.

In the second experiment, we evaluate the effect of dividing the image into multiple rectangle patches in (sd2D), quantizing and reconstructing the image individually using the test image Lena. The process can be done in parallel, which makes the decoding process significantly faster than the single patch 2D reconstruction. As shown in Figure 7, there's usually no visible difference between using 1 patch and multiple patches in quantization and reconstruction. In both cases, the images look more natural and closer to the original image than MSQ, as the latter is unable to distinguish the subtle difference between pixels, especially in the face and shoulder area.

To further investigate where the improved PSNRs of the two Sigma Delta reconstructions come from, we plot the absolute spectra of the three reconstructions in Figure 8 as well as the absolute spectra of the residue images in Figure 10. The residue image (Figure 9) is defined as the difference between the reconstructed image and the original image. From Figure 10, we see that as predicted, our decoders can indeed retain the high frequency information while effectively compressing the low frequency noise.

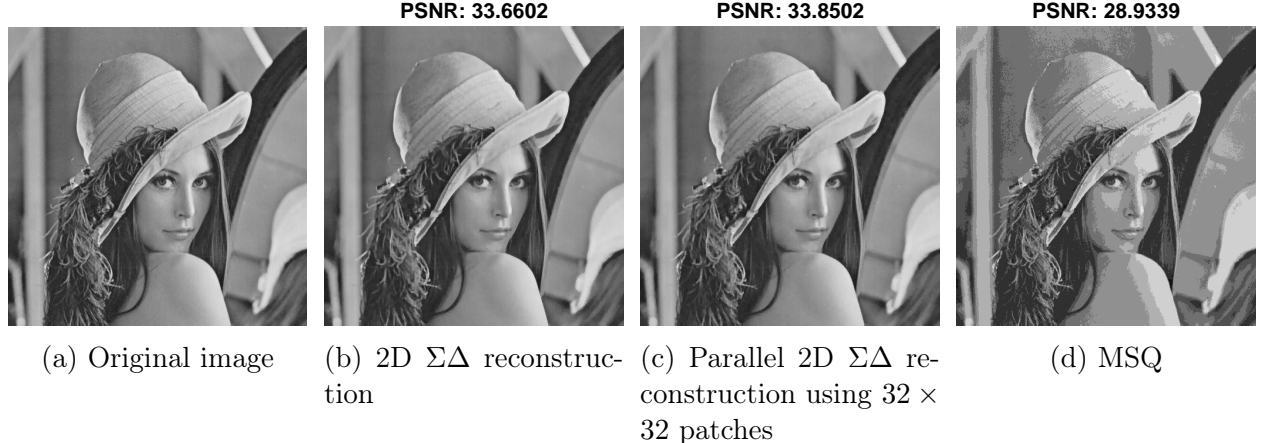


Figure 7: Reconstruction results of 2D  $\Sigma\Delta$ , 2D parallel  $\Sigma\Delta$  and MSQ quantization, here we used 3-bit quantization in both  $\Sigma\Delta$  and MSQ cases.

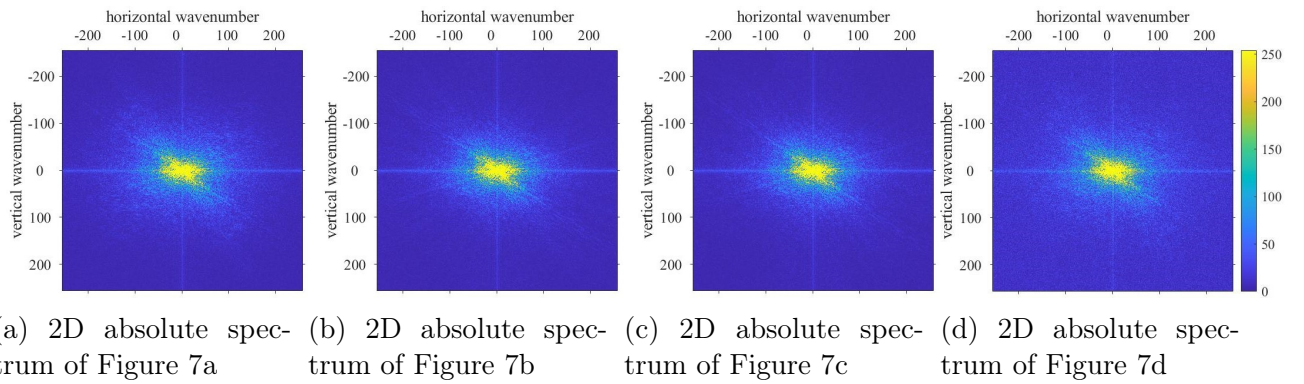
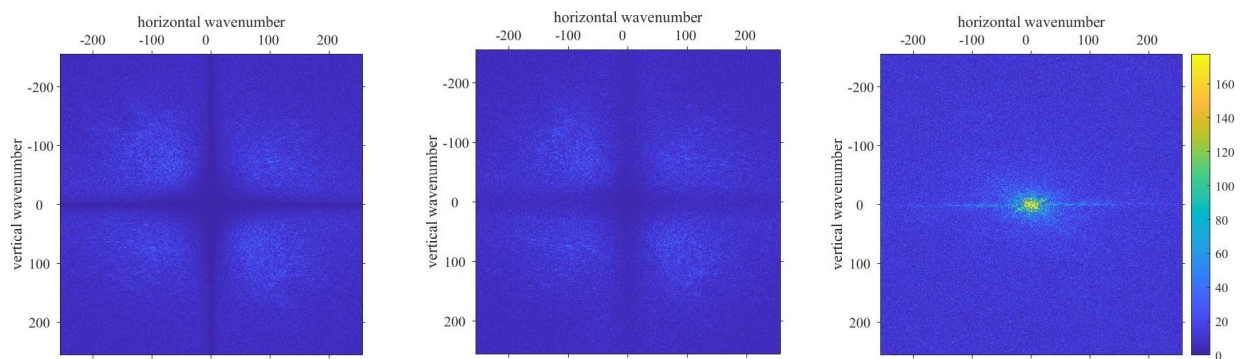


Figure 8: Comparison of the 2D absolute spectra of the images in Figure 7, from left to right are absolute spectrum of the true image, that of the 2D single patch  $\Sigma\Delta$  reconstruction, that of the 2D  $32 \times 32$  patch  $\Sigma\Delta$  reconstruction, and that of the MSQ, respectively. The sub-figures share the same colormap.



(a) Residue image of Figure 7b (b) Residue image of Figure 7c (c) Residue image of Figure 7d

Figure 9: Comparison of residue images in Figure 7. From left to right are residue of the 2D single patch  $\Sigma\Delta$  reconstruction, residue of the 2D  $32 \times 32$  patch  $\Sigma\Delta$  reconstruction, and that of the MSQ, respectively.



(a) 2D absolute spectrum of Figure 9a (b) 2D absolute spectrum of Figure 9b (c) 2D absolute spectrum of Figure 9c

Figure 10: Comparison of the 2D absolute spectra of the residue images in Figure 9. From left to right are 2D single patch  $\Sigma\Delta$  reconstruction, 2D  $32 \times 32$  patch  $\Sigma\Delta$  reconstruction, and MSQ, respectively.

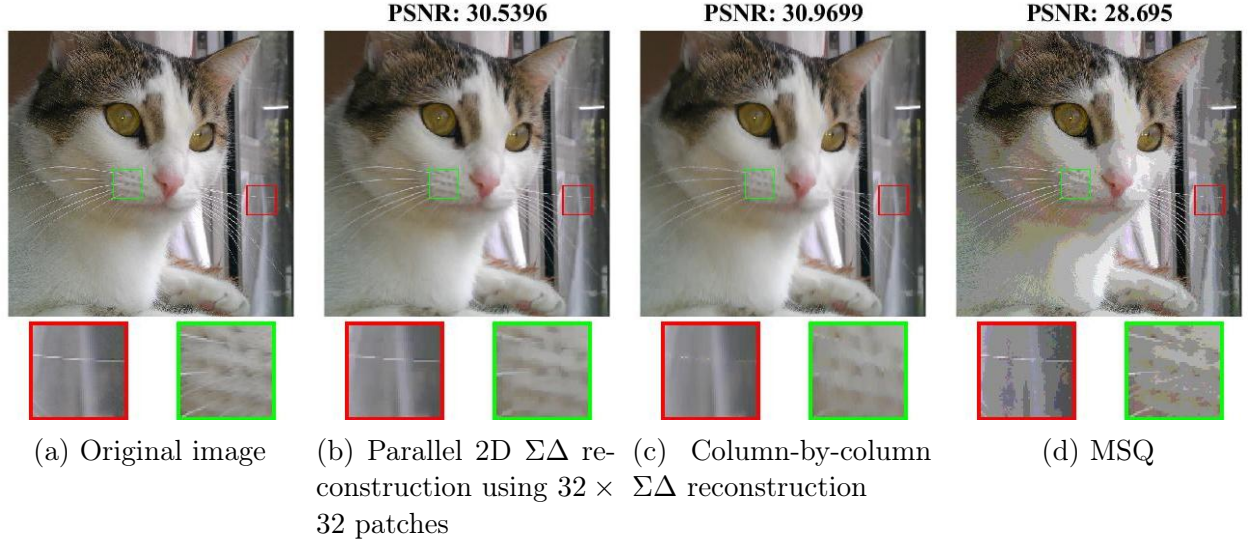


Figure 11: Reconstruction results of RGB image, here we used 3-bit quantization in both  $\Sigma\Delta$  and MSQ cases.

Next, we test the performance of the proposed decoder on RGB images.

Figure 11 shows that compared with MSQ, the proposed  $\Sigma\Delta$  reconstructions did a better job at preserving the original color and getting rid of the halos. Similar to the gray-scale image case (Figure 6), the 2D  $\Sigma\Delta$  quantization captured more horizontal structure than the column by column  $\Sigma\Delta$  quantization.

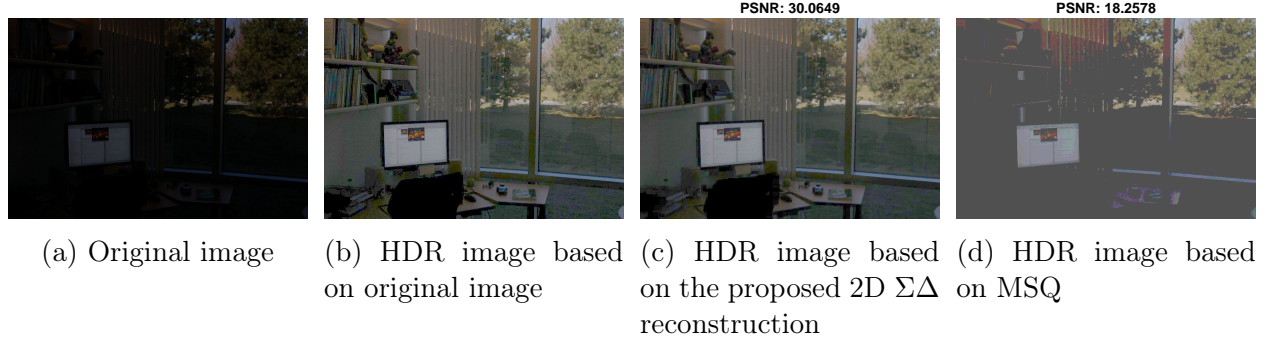


Figure 12: HDR reconstruction results, here we used 4-bit quantization in both  $\Sigma\Delta$  and MSQ cases. (a): the ground truth. (b): HDR image from the ground truth. (c): HDR image from the proposed  $\Sigma\Delta$  reconstruction, we used  $Q_{2D}$  and decoder (2.6). (d): HDR image from MSQ quantization.

In the last experiment, we demonstrate that the proposed scheme can greatly enhance image quality captured in a dark environments. A well known problem with current cameras is when shooting in dark environment and with short exposure time, the CMOS sensors will return a ‘dark’ image like the one in Figure 12 (a). Technically, the dark images are those

with low Dynamic Range (DR), i.e., the ratio between the maximum and minimum light intensities. A typical way to correct the dynamical range is through post-processing. For example, if we use the formula  $X(i, j) = X(i, j)^{1/3}$  to adjust the brightness, Figure 12 (a) becomes Figure 12 (b), which has a high image quality. However, in practice, one always needs to do quantization once Figure 12 (a) is captured. If the brightness adjustment is performed on the quantized image, the resulting image Figure 12 (d) looks much worse. We found that with the same number of bits, if we just replace MSQ with the proposed Sigma Delta quantization, we can get a significantly improvement Figure 12 (c), where the hidden details in the dark scene were revealed much better. This observation indicates that the proposed scheme might be especially promising for taking pictures in the dark environment.

### Acknowledgements

The authors are supported by the NSF grant CCF-1909523.

## References

- [1] H. Alzer and S. Koumandos. Sharp inequalities for trigonometric sums in two variables. 2004.
- [2] R. G. Baraniuk, S. Foucart, D. Needell, Y. Plan, and M. Wootters. Exponential decay of reconstruction error from binary measurements of sparse signals. *IEEE Transactions on Information Theory*, 63(6):3368–3385, 2017.
- [3] J. J. Benedetto, A. M. Powell, and Ö. Yilmaz. Sigma-delta ( $\Sigma\Delta$ ) quantization and finite frames. *IEEE Trans. Inf. Theory*, 52(5):1990–2005, 2006.
- [4] S. Bernstein. *Sur l’ordre de la meilleure approximation des fonctions continues par des polynômes de degré donné*, volume 4. Hayez, imprimeur des académies royales, 1912.
- [5] J. Blum, M. Lammers, A. M. Powell, and Ö. Yilmaz. Sobolev duals in frame theory and sigma-delta quantization. *J. Fourier Anal. Appl.*, 16(3):365–381, 2010.
- [6] B. G. Bodmann and V. I. Paulsen. Frame paths and error bounds for sigma-delta quantization. *Applied and Computational Harmonic Analysis*, 22(2):176–197, 2007.
- [7] P. T. Boufounos and R.G. Baraniuk. Quantization of sparse representations. In *2007 Data Compression Conference (DCC’07)*, pages 378–378. IEEE, 2007.
- [8] S. Boyd, N. Parikh, E. Chu, B. Peleato, and J. Eckstein. Distributed optimization and statistical learning via the alternating direction method of multipliers. *Foundations and Trends® in Machine learning*, 3(1):1–122, 2011.
- [9] E. J. Candès and C. Fernandez-Granda. Super-resolution from noisy data. *Journal of Fourier Analysis and Applications*, 19(6):1229–1254, 2013.

- [10] E. J. Candès and C. Fernandez-Granda. Towards a mathematical theory of super-resolution. *Communications on pure and applied Mathematics*, 67(6):906–956, 2014.
- [11] A. Chambolle and T. Pock. A first-order primal-dual algorithm for convex problems with applications to imaging. *Journal of mathematical imaging and vision*, 40(1):120–145, 2011.
- [12] E. Chou. *Beta-duals of frames and applications to problems in quantization*. PhD thesis, New York University, 2013.
- [13] E. Chou and C. S. Güntürk. Distributed noise-shaping quantization: I. Beta duals of finite frames and near-optimal quantization of random measurements. *Constructive Approximation*, 44(1):1–22, 2016.
- [14] E. Chou and C. S. Güntürk. Distributed noise-shaping quantization: II. Classical frames. In *Excursions in Harmonic Analysis, Volume 5*, pages 179–198. Springer, 2017.
- [15] E. Chou, C. S. Güntürk, F. Krahmer, R. Saab, and Ö. Yilmaz. Noise-shaping quantization methods for frame-based and compressive sampling systems. In *Sampling theory, a renaissance*, pages 157–184. Springer, 2015.
- [16] I. Daubechies and R. DeVore. Approximating a bandlimited function using very coarsely quantized data: a family of stable sigma-delta modulators of arbitrary order. *Ann. Math.*, 158(2):679–710, 2003.
- [17] P. Deift, C. S. Güntürk, and F. Krahmer. An optimal family of exponentially accurate one-bit sigma-delta quantization schemes. *Comm. Pure Appl. Math.*, 64(7):883–919, 2011.
- [18] S. Dirksen, H. C. Jung, and H. Rauhut. One-bit compressed sensing with partial gaussian circulant matrices. *arXiv preprint arXiv:1710.03287*, 2017.
- [19] S. Dirksen and A. Stollenwerk. Fast binary embeddings with gaussian circulant matrices: improved bounds. *Discrete & Computational Geometry*, 60(3):599–626, 2018.
- [20] J.-M. Feng, F. Krahmer, and R. Saab. Quantized compressed sensing for partial random circulant matrices. In *2017 International Conference on Sampling Theory and Applications (SampTA)*, pages 236–240. IEEE, 2017.
- [21] V. K. Goyal, M. Vetterli, and N. T. Thao. Quantized overcomplete expansions in  $\mathbb{R}^n$ : analysis, synthesis, and algorithms. *IEEE Transactions on Information Theory*, 44(1):16–31, 1998.
- [22] C. S. Güntürk. One-bit sigma-delta quantization with exponential accuracy. *Comm. Pure Appl. Math.*, 56(11):1608–1630, 2003.

- [23] C. S. Güntürk, M. Lammers, A. M. Powell, R. Saab, and Ö. Yilmaz. Sobolev duals for random frames and sigma-delta quantization of compressed sensing measurements. *Foundations of Computational mathematics*, 13(1):1–36, 2013.
- [24] C. S. Güntürk and W. Li. High-performance quantization for spectral super-resolution. *arXiv preprint arXiv:1902.00131*, 2019.
- [25] T. Huynh and R. Saab. Fast binary embeddings and quantized compressed sensing with structured matrices. *Communications on Pure and Applied Mathematics*, 73(1):110–149, 2020.
- [26] H. Inose and Y. Yasuda. A unity bit coding method by negative feedback. *Proceedings of the IEEE*, 51(11):1524–1535, 1963.
- [27] L. Jacques, J. N. Laska, P. T. Boufounos, and R. G. Baraniuk. Robust 1-bit compressive sensing via binary stable embeddings of sparse vectors. *IEEE Trans. Inf. Theory*, 59(4):2082–2102, 2013.
- [28] F. Krahmer, R. Saab, and R. Ward. Root-exponential accuracy for coarse quantization of finite frame expansions. *IEEE Trans. Inf. Theory*, 58(2):1069 –1079, February 2012.
- [29] F. Krahmer, R. Saab, and Ö Yilmaz. Sigma–delta quantization of sub-gaussian frame expansions and its application to compressed sensing. *Information and Inference: A Journal of the IMA*, 3(1):40–58, 2014.
- [30] M. Lammers, A. M. Powell, and Ö. Yilmaz. Alternative dual frames for digital-to-analog conversion in sigma–delta quantization. *Advances in Computational Mathematics*, 32(1):73, 2010.
- [31] W. Li. Elementary  $l^\infty$  error estimates for super-resolution de-noising. *arXiv preprint arXiv:1702.03021*, 2017.
- [32] E. Lybrand and R. Saab. Quantization for low-rank matrix recovery. *Information and Inference: A Journal of the IMA*, 8(1):161–180., 2019.
- [33] F. Krahmer P. T. Boufounos, L. Jacques and R. Saab. Quantization and compressive sensing. In *Compressed sensing and its applications*, pages 193–237. Springer, 2015.
- [34] Y. Plan and R. Vershynin. Robust 1-bit compressed sensing and sparse logistic regression: A convex programming approach. *IEEE Transactions on Information Theory*, 59(1):482–494, 2012.
- [35] Y. Plan and R. Vershynin. Dimension reduction by random hyperplane tessellations. *Discrete & Computational Geometry*, 51(2):438–461, 2014.
- [36] A. M. Powell, R. Saab, and Ö. Yilmaz. Quantization and finite frames. In *Finite frames*, pages 267–302. Springer, 2013.

- [37] L. Roberts. Picture coding using pseudo-random noise. *IRE Transactions on Information Theory*, 8(2):145–154, 1962.
- [38] R. Saab, R. Wang, and Ö Yilmaz. From compressed sensing to compressed bit-streams: practical encoders, tractable decoders. *IEEE Transactions on Information Theory*, 64(9):6098–6114, 2017.
- [39] R. Saab, R. Wang, and Ö Yilmaz. Quantization of compressive samples with stable and robust recovery. *Applied and Computational Harmonic Analysis*, 44(1):123–143, 2018.
- [40] R. Schreier and G. C. Temes. *Understanding delta-sigma data converters*, volume 74. IEEE press Piscataway, NJ, 2005.
- [41] L. Schuchman. Dither signals and their effect on quantization noise. *IEEE Transactions on Communication Technology*, 12(4):162–165, 1964.
- [42] R. Wang. Sigma delta quantization with harmonic frames and partial fourier ensembles. *Journal of Fourier Analysis and Applications*, 24(6):1460–1490, 2018.

## 6 Appendix

**Lemma 6.1.** [modified Lemma 2.4 [9]] Suppose  $T = \{t_1, t_2, \dots, t_s\} \subset [0, 1]$  satisfies minimum separation condition, i.e.,  $\min_{t, t' \in T, t \neq t'} |t - t'| \geq \frac{2}{M}$ ,  $v \in \mathbb{C}^{|T|}$  is arbitrary vector with  $|v_j| = 1, j = 1, 2, \dots, s$ . Then there exists a low-frequency trigonometric polynomial

$$q(t) = \sum_{k=-M}^M c_k e^{i2\pi k t}, \quad t \in [0, 1]$$

obeying the following properties:

$$q(t_j) = v_j, \quad t_j \in T$$

$$|q(t)| \leq 1 - C_a M^2 (t - t_j)^2, \quad t \in S_M(j)$$

$$|q(t)| < 1 - C_b, \quad t \in S_M^c$$

with  $0 < C_b \leq 0.16^2 C_a < 1$ .